The Journal of Experimental Biology 213, 3559-3574
© 2010. Published by The Company of Biologists Ltd
doi:10.1242/jeb.041228

The proteomic response of the mussel congeners *Mytilus galloprovincialis* and *M. trossulus* to acute heat stress: implications for thermal tolerance limits and metabolic costs of thermal stress

Lars Tomanek* and Marcus J. Zuzow

California Polytechnic State University, Department of Biological Sciences, Center for Coastal Marine Sciences, Environmental Proteomics Laboratory, 1 Grand Avenue, San Luis Obispo, CA 93407-0401, USA

*Author for correspondence (ltomanek@calpoly.edu)

Accepted 2 August 2010

SUMMARY

The Mediterranean blue mussel, *Mytilus galloprovincialis*, an invasive species in California, has displaced the more heat-sensitive native congener, *Mytilus trossulus*, from its former southern range, possibly due to climate change. By comparing the response of their proteomes to acute heat stress we sought to identify responses common to both species as well as differences that account for greater heat tolerance in the invasive. Mussels were acclimated to 13°C for four weeks and exposed to acute heat stress (24°C, 28°C and 32°C) for 1 h and returned to 13°C to recover for 24 h. Using two-dimensional gel electrophoresis and tandem mass spectrometry we identified 47 and 61 distinct proteins that changed abundance in *M. galloprovincialis* and *M. trossulus*, respectively. The onset temperatures of greater abundance of some members of the heat shock protein (Hsp) 70 and small Hsp families were lower in *M. trossulus*. The abundance of proteasome subunits was lower in *M. galloprovincialis* but greater in *M. trossulus* in response to heat. Levels of several NADH-metabolizing proteins, possibly linked to the generation of reactive oxygen species (ROS), were lower at 32°C in the cold-adapted *M. trossulus* whereas proteins generating NADPH, important in ROS defense, were higher in both species. The abundance of oxidative stress proteins was lower at 32°C in *M. trossulus* only, indicating that its ability to combat heat-induced oxidative stress is limited to lower temperatures. Levels of NAD-dependent deacetylase (sirtuin 5), which are correlated with lifespan, were lower in *M. trossulus* in response to heat stress. In summary, the expression patterns of proteins involved in molecular chaperoning, proteolysis, energy metabolism, oxidative damage, cytoskeleton and deacetylation revealed a common loci of heat stress in both mussels but also showed a lower sensitivity to high-temperature damage in the warm-adapted *M. galloprovincialis*, which is consistent with its expanding range in warmer waters.

Supplementary material available online at http://jeb.biologists.org/cgi/content/full/213/20/3559/DC1

Key words: biogeography, climate change, heat stress, *Mytilus galloprovincialis*, *Mytilus trossulus*, proteomics, systems biology, temperature.

INTRODUCTION

Temperature plays an important role in setting limits to the distributions of marine organisms due to its ubiquitous effects on the rates of physiological processes and the integrity of macromolecular cellular structures (Hochachka and Somero, 2002). Recent increases in temperatures due to global climate change (IPCC, 2007) have already led to shifts in biogeographic ranges in a number of marine and terrestrial organisms (Harley et al., 2006; Parmesan, 2006). In order to predict the effects of increasing temperatures we need to know the energetic costs of short- and long-term thermal stress among species that occupy different thermal environments. A number of physiological processes have been proposed to be important indicators of thermal stress, e.g. the synthesis of molecular chaperones that stabilize denaturing proteins, and a mismatch between oxygen supply and demand (Hochachka and Somero, 2002; Pörtner, 2002). These have been shown to be potentially useful for predicting the effects of global climate change on shifting species' ranges in the marine environment (Pörtner and Knust, 2007; Somero, 2010; Stillman, 2003; Tomanek, 2008; Tomanek, 2010; Tomanek and Somero, 1999). Recently, several transcriptomic studies have applied a systems biology approach and discovered novel indicators of thermal stress by simultaneously assessing the changes in the expression of the mRNA of thousands of genes (Gracey et al., 2008; Place et al., 2008; Podrabsky and Somero, 2004; Stillman and Tagmount, 2009; Teranishi and Stillman, 2007). However, to our knowledge, there has not been a comparison of the proteomic changes in response to heat stress in marine organisms that differ in thermotolerance and distribution, which could provide insights into systemic changes beyond the transcriptome.

We chose the blue mussel species pair *Mytilus galloprovincialis* and *Mytilus trossulus* for a comparison of the proteomic changes in response to acute heat stress. The latter species is the ancestral species from the North Pacific that gave rise to the North Atlantic *Mytilus edulis*, which then gave rise to the Mediterranean *M. galloprovincialis* (Seed, 1992). At some point in the last century, the Mediterranean species was introduced to southern California through shipping (McDonald and Koehn, 1988) and has since replaced the native *M. trossulus* along the southern half of the Californian coast up to the latitude of Monterey Bay (Geller, 1999). The coast between Monterey Bay and San Francisco Bay is currently a hybrid zone (Braby and Somero, 2006a) but single-species populations of *M. trossulus* are found along the coast north of San Francisco Bay. Evidence from field surveys of patterns of species abundance (Schneider, 2008) and thermal stress, heart rate measurements (Braby and Somero, 2006b), heat shock protein (Hsp) synthesis, formation of ubiquitin conjugates (Hofmann and Somero, 1996a) and enzyme function (Fields et al., 2006) all suggest that *M. galloprovincialis* is a more warm-adapted species than *M. trossulus*. Although it is likely that the range expansion of *M. galloprovincialis* and the replacement of *M. trossulus* are determined by a number of interacting abiotic and biotic factors, temperature has been shown to play an important role in driving patterns of selection between these congeners and contributing to setting the current species' ranges (Braby and Somero, 2006a; Schneider and Helmuth, 2007).

A number of studies have started to characterize the proteomic response of *Mytilus* congeners to stresses, such as oxidative stress and pollutant exposure (Apraiz et al., 2006; McDonagh and Sheehan, 2007). Other studies have focused on the variation in the proteome in eggs and hybrids (Diz and Skibinski, 2007) or compared *M. edulis* with *M. galloprovincialis* acclimatized to temperature conditions of their respective geographic ranges (López et al., 2002). However, the present study is the first comprehensive comparison of the proteomic response to acute heat stress between any pair of *Mytilus* congeners, notably a pair whose biogeographic ranges are in flux.

We used a proteomics approach based on two-dimensional gel electrophoresis (2-D GE) to provide a global perspective on how protein abundance changes, either due to changes in expression (i.e. synthesis), post-translational modifications (PTMs) or degradation in response to heat stress in the two mussel congeners. Using an expressed sequence tag (EST) library generated by various transcriptomic projects (Gracey et al., 2008; Lockwood et al., 2010) and tandem mass spectrometry (MS), we were able to identify a number of proteins that showed differential expression profiles in response to acute heat shock.

MATERIALS AND METHODS

Animal collection and maintenance

Mytilus galloprovincialis (Lamarck 1819) was collected subtidally from Santa Barbara, CA, USA (34°24′15″N, 119°41′30″W), and *Mytilus trossulus* (Gould 1850) from Newport, OR, USA (44°38′25″N, 124°03′10″W). Species identities were confirmed at both sites using PCR (Lockwood et al., 2010). Animals were kept for four weeks at 13°C in recirculating seawater tanks and fed a phytoplankton diet every day.

Experimental design

Mussels were placed in a temperature-controlled ice chest with circulating seawater and aeration. The temperature was increased by 6°C h^{-1} from 13°C to 24°C, 28°C or 32°C. Mussels were kept at these temperatures for 1 h and subsequently brought back to 13°C for a 24 h recovery period. Gill tissues were sampled from all treatment groups (*N*=6 for all groups) and the 13°C control group within a 1.5 h period following the 24 h recovery period to avoid any possible differences due to circadian or circatidal rhythms and subsequently kept at –80°C. In addition, tissues of other mussels were sampled immediately following heat stress (0 h recovery) for transcriptomic analysis (Lockwood et al., 2010).

Homogenization

Frozen gill tissue was thawed and lysed in a ratio of 1:4 of tissue to homogenization buffer [7 mol l^{-1} urea, 2 mol l^{-1} thiourea, 1% ASB-14 (amidosulfobetaine-14), 40 mmol l^{-1} Tris-base, 0.5% immobilized pH 4–7 gradient (IPG) buffer (GE Healthcare, Piscataway, NJ, USA) and 40 mmol l^{-1} dithiothreitol], using an ice-cold ground-glass homogenizer. The homogenate was subsequently centrifuged at room temperature for 30 min at 16,100 ***g*** and the supernatant was used for further processing. Proteins of the supernatant were precipitated by adding four volumes of ice-cold 10% trichloroacetic acid in acetone and incubating the solution at –20°C overnight. After centrifugation at 4°C for 15 min at 18,000 ***g***, the supernatant was discarded and the remaining pellet was washed with ice-cold acetone, and centrifuged again before being re-suspended in rehydration buffer [7 mol l^{-1} urea, 2 mol l^{-1} thiourea, 2% CHAPS (cholamidopropyl-dimethylammonio-propanesulfonic acid), 2% NP-40 (nonyl phenoxylpolyethoxylethanol-40), 0.002% Bromophenol Blue, 0.5% IPG buffer and 100 mmol l^{-1} dithioerythritol] through vortexing. The protein concentration was determined with the 2D Quant kit (GE Healthcare), according to the manufacturer's instructions.

Two-dimensional gel electrophoresis

Proteins (400 μg) were loaded onto IPG strips (pH 4–7, 11 cm; GE Healthcare) for separation according to their isoelectric point (pI). We started the isoelectric focusing protocol with a passive rehydration step (5 h), followed by 12 h of active rehydration (50 V), using an isoelectric focusing cell (BioRad, Hercules, CA, USA). The following protocol was used for the remainder of the run (all voltage changes occurred in rapid mode): 500 V for 1 h, 1000 V for 1 h, and 8000 V for 2.5 h. The strips were frozen at –80°C.

Frozen strips were thawed and incubated in equilibration buffer [375 mmol l^{-1} Tris-base, 6 mol l^{-1} urea, 30% glycerol, 2% SDS (sodium dodecyl sulfate) and 0.002% Bromophenol Blue] for 15 min, first with 65 mmol l^{-1} dithiothreitol and then, second with 135 mmol l^{-1} iodoacetamide. IPG strips were placed on top of a 12% polyacrylamide gel with a 0.8% agarose solution containing Laemmli SDS electrophoresis (or running) buffer (25 mmol l^{-1} Tris-base, 192 mmol l^{-1} glycine and 0.1% SDS). Gels were run (Criterion Dodeca; BioRad) at 200 V for 55 min with a recirculating water bath set at 10°C. Gels were subsequently stained with colloidal Coomassie Blue (G-250) overnight and destained by washing repeatedly with Milli-Q (Millipore, Billerica, MA, USA) water for 48 h. The resulting gel images were scanned with a transparency scanner (model 1280; Epson, Long Beach, CA, USA).

Gel image analysis

Digitized images of two-dimensional gels were analyzed using Delta2D (version 3.6; Decodon, Greifswald, Germany) (Berth et al., 2007). We used the group warping strategy to connect gel images through match vectors. All images within a species were fused into a composite image (=proteome map), which represents mean volumes for each spot (Fig. 1). Spot boundaries were detected within the proteome map and transferred back to all gel images using match vectors. After background subtraction, protein spot volumes were normalized against total spot volume of all proteins in a gel image.

Mass spectrometry

Proteins that changed in abundance in response to heat shock were excised from gels using a tissue puncher (Beecher Instruments, Prairie, WI, USA). Gel plugs were destained twice with 25 mmol l^{-1} ammonium bicarbonate in 50% acetonitrile, dehydrated with 100% acetonitrile and digested with 11 ng μl^{-1} of trypsin (Promega, Madison, WI, USA) overnight at 37°C. Digested proteins were extracted using elution buffer [0.1% trifluoroacetic acid (TFA)/ acetonitrile; 2:1] and concentrated using a SpeedVac (Thermo Fisher Scientific, Waltham, MA, USA). The elution buffer containing the digested protein was mixed with 5 μl of matrix

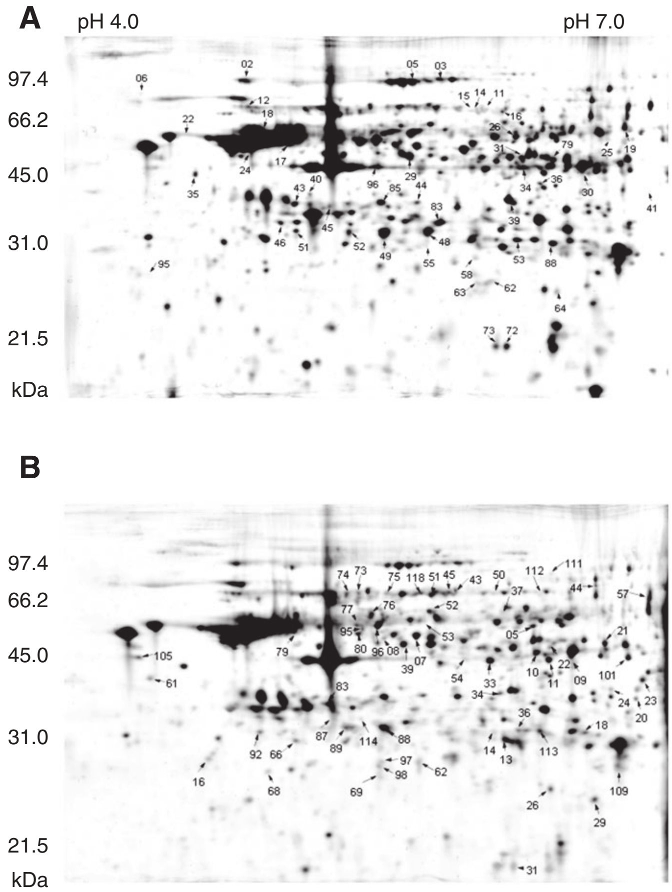

Fig. 1. Two composite gel images (or proteome maps) depicting 554 and 465 protein spots from gill tissue of the blue mussel species *Mytilus galloprovincialis* (A) and *Mytilus trossulus* (B), respectively, from all gels of the treatment within one species. The proteome maps represent average pixel volumes for each protein spot. Numbered spots were those that showed changes in abundance in response to acute heat stress treatments (one-way ANOVA, $P<0.02$) and were identified using tandem mass spectrometry (for identifications, see Tables S1 and S2).

solution (0.2 mg ml^{-1} α-hydroxycyano cinnamic acid in acetonitrile) and spotted on an Anchorchip$^{\mathrm{TM}}$ target plate (Bruker Daltonics Inc., Billerica, MA, USA). The spotted proteins were washed with 0.1% TFA and recrystalized using an acetone/ethanol/0.1% TFA (6:3:1) mixture.

Peptide mass fingerprints (PMFs) were obtained on a matrix-assisted laser desorption ionization tandem time-of-flight (MALDI-TOF-TOF) mass spectrometer (Ultraflex II; Bruker Daltonics Inc.). We chose a minimum of six peptides to conduct tandem MS in order to obtain information about the b- and y-ions of the peptide sequence.

To analyze the peptide spectra we used flexAnalysis (version 3.0; Bruker Daltonics Inc.) and applied the TopHat algorithm for baseline subtraction, the Savitzky–Golay analysis for smoothing (with: 0.2 *m*/*z*; number of cycles=1) and the SNAP algorithm to detect peaks (signal-to-noise ratio: 6 for MS and 1.5 for MS/MS). The charge state of the peptides was assumed to be +1. We used porcine trypsin for internal mass calibration.

To identify proteins we used Mascot (version 3.1; Matrix Science Inc., Boston, MA, USA) and combined PMFs and tandem mass spectra in a search against two databases. One database is an EST library that initially contained approximately 26,000 entries, which represented 12,961 and 1688 different gene sequences for *Mytilus californianus* and *M. galloprovincialis*, respectively (Lockwood et al., 2010). The other one was Swiss-Prot (last update: June 2009) with 17,360 molluskan protein sequences. Oxidation of methionine and carbamidomethylation of cysteine were our only variable modifications. Our search allowed one missed cleavage during trypsin digestion. For tandem MS we set the precursor ion mass tolerance to 0.6 Da. The molecular weight search (MOWSE) score that indicated a significant hit was dependent on the database: scores higher than 43 and 24 were significant ($P<0.05$) in a search in the *Mytilus* EST and Swiss-Prot database, respectively. However, we only accepted positive identifications that included two matched peptides regardless of the MOWSE score (supplementary material Tables S1 and S2).

Statistical analysis

Normalized spot volumes were analyzed within Delta2D (version 3.6; Decodon, Greifswald, Germany) by using an analysis of variance (one-way ANOVA) within each species and with temperature as the main effect. For the one-way ANOVA a null distribution was generated using 1000 permutations to account for the unequal variance and non-normal distributions of the response variables, and a *P*-value of 0.02 was used to limit the number of false positives instead of using a multiple-comparison correction. A two-way ANOVA was not possible because a number of gel regions were difficult to match between species, and even for those proteins that overlapped between species it was unclear whether proteins were orthologous or paralogous homologs. Following the one-way ANOVA, *post-hoc* testing to compare treatments was conducted using Tukey's analysis ($P<0.05$), using Minitab (version 15; Minitab Inc., State College, PA, USA). For the hierarchical clustering we used average linking within the statistical tool suite within Delta2D, using a Pearson's correlation metric. We also used a principle component analysis (PCA) within Delta2D to assess the contribution of temperature to the variation in protein abundance patterns. For the same reasons as to why we were unable to conduct a two-way ANOVA, the PCA had to be conducted within species and compared afterwards. The results of the PCA comparing temperature treatments within each species were interpreted with the help of loading plots; we used these plots to assess which proteins contributed the most to the component of interest.

RESULTS AND DISCUSSION

Criteria for comparing proteomes between species

To our knowledge this is the first comparison of the proteomic response of two closely related, yet differently thermally adapted, marine species to acute heat stress. Changes in protein abundance occur due to protein synthesis, PTMs or degradation. Thus, when we use the terms abundance, levels or up- and down-regulation, we do it in a broad sense that may encompass all three of these processes.

Comparisons of changes in proteomes, even between such closely related species, pose conceptual challenges because of evolutionary variation in primary sequence and PTMs of orthologous homologs, which can lead to changes in the molecular mass and pI of protein isoforms after separation with 2-D GE. Thus, it is necessary to explicitly state the criteria for comparing protein expression profiles between species.

First, the ideal comparison of levels of protein abundance is between proteins that are orthologous homologs and have overlapping positions on a 2-D gel image, e.g. isoforms that are identical on the level of the primary amino acid sequence and either lack or have identical PTMs. However, comparisons of spots from the same position, even between closely related species, may not be assumed to involve homologs without identification with MS. Most of the identified Hsp70 isoforms, the two major small Hsps (sHsps) and several of the proteasome isoforms match this criterion and thus can directly be compared.

Second, even a single amino acid substitution or PTM can cause a shift in pI without greatly changing the molecular mass of a protein in a gel. Thus, it is very likely that isoforms with the same protein identification and of similar molecular mass but different pI are homologous between the congeners. However, estimated and predicted molecular masses of proteins identified can differ (supplementary material Tables S1 and S2), because the accuracy of the estimated molecular mass is based on 2-D gels (Fig. 1) and our identifications are based on EST library entries whose predicted masses are often based on homologs that are from a phylogenetically distant species. It is important that the deviations are not biased towards one way, e.g. consistently lower values would indicate that protein degradation was occurring.

Third, proteins that change intensity but were only identified in one congener require a more cautious interpretation that considers the possibility that the homolog either did not change in abundance and thus did not get prepared for MS analysis or that it varies enough in pI that it is outside the pH range analyzed (pH 4–7). Additionally, protein levels could also be too low to be easily detected in the congener where the protein was not found to change. However, identification of two or more proteins belonging to the same cellular pathway in one but not the other congener is strongly suggestive of interspecific differences. Thus, some interspecific differences presented here are treated as conclusive while others should be considered as hypotheses that are more speculative.

In the following sections we will first focus on changes in protein abundance within species according to protein function. Within each section we will point out differences in protein abundance between species as well as indicating where the transcriptomic analysis (Lockwood et al., 2010) concurs or diverges from our results. We will then synthesize these results into three hypotheses on the changes in protein abundance that may occur during heat stress

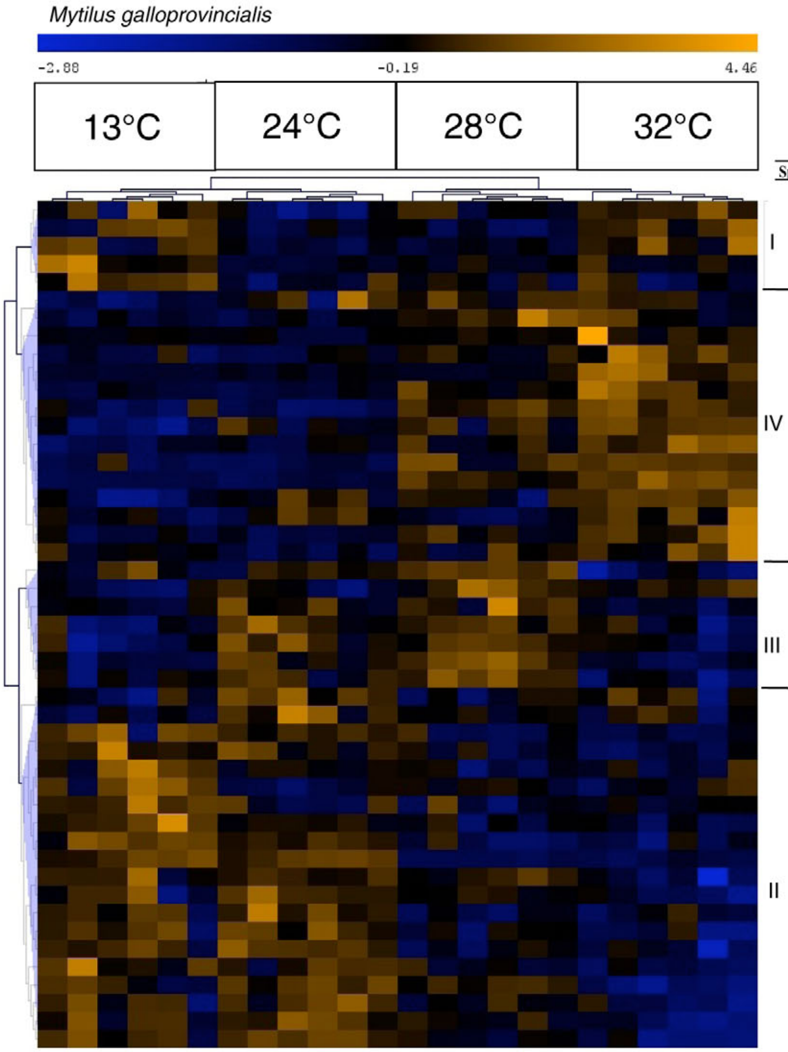

Spot ID	Protein ID	Functional Category
88	Actin	cytoskeletal
46	α-Tubulin	cytoskeletal
96	Actin	cytoskeletal
34	Phosphoenol pyruvate carboxykinase	energy metabolism
30	Isocitrate dehydrogenase (NADP)	energy metabolism
83	α-crystalline-Hsp23	molecular chaperones
11	Hsp70	molecular chaperones
64	Proteasome β-type 6	protein degradation
52	α-crystalline-Hsp23	molecular chaperones
14	Hsp70	molecular chaperones
15	Hsp70	molecular chaperones
63	Ras-like GTP-binding protein RhoA	signaling
36	Isocitrate dehydrogenase (NADP)	energy metabolism
49	α-crystalline-Hsp23	molecular chaperones
48	Hsp27	molecular chaperones
73	Cu-Zn Superoxide dismutase	oxidative stress
35	Ribosomal protein 2S	protein sythesis
16	Hsp70	molecular chaperones
55	6-Phospho-glucono lactonase	pentose phosphate
6	Major vault protein	unspecified
26	β-Tubulin	cytoskeletal
22	β-Tubulin	cytoskeletal
95	β-Tubulin	cytoskeletal
2	Hsp90	molecular chaperones
24	β-Tubulin	cytoskeletal
17	α-Tubulin	cytoskeletal
18	α-Tubulin	cytoskeletal
19	Thiamine pyrophosphate transketolase	pentose phosphate
12	Hsc70	molecular chaperones
41	Arginine kinase	energy metabolism
31	Aspartate amino transferase	energy metabolism
43	Pyrophosphatase	energy metabolism
53	Proteasome α-type 6	protein degradation
79	Isocitrate dehydrogenase (NADP)	energy metabolism
51	Proteasome β-type 3	protein degradation
62	Proteasome β-type 2	protein degradation
72	Cu-Zn Superoxide dismutase	oxidative stress
39	cytosolic Malate dehydrogenase	energy metabolism
29	Gelsolin	cytoskeletal
25	β-Tubulin	cytoskeletal
3	Major vault protein	unspecified
5	Major vault protein	unspecified
58	Nucleoside diphosphate kinase	energy metabolism
44	G-protein β-subunit	signaling
85	G-protein β-subunit	signaling
45	Proteasome α-type 1	protein degradation
40	α-Tubulin	cytoskeletal

Fig. 2. Hierarchal clustering of identified proteins using Pearson's correlation in response to acute heat stress in the warm-adapted *Mytilus galloprovincialis*. Blue coloring represents a lower than average standardized volume whereas orange represents greater than average standardized volume. The horizontal axis shows the different temperature treatments. The vertical axis represents the standardized expression patterns of the identified proteins. The clustering shows four major groups of proteins with similar expression patterns (labeled I–IV).

within a species. Finally, using these three hypotheses we will summarize the interspecific differences between the two *Mytilus* congeners.

Molecular chaperones

Levels of isoforms of the heat shock protein 70 (Hsp70) and sHsp families were higher in response to heat stress in both congeners (Figs 2–5). We identified four inducible Hsp70 isoforms in *M. galloprovincialis*, all concentrated around pH 6.0 (Figs 2 and 4). One was higher at 28°C, the others at 32°C, relative to the 13°C control. A fifth isoform was identified as an Hsp70 cognate, Hsc70, which was higher at 24°C only. In *M. trossulus* we identified nine Hsp70 isoforms, one of them at a lower molecular mass than 70 kDa (spot 54; Figs 3 and 4). Four (spots 43, 45, 51 and 118) were in a cluster similar to the four Hsp70 isoforms in *M. galloprovincialis* but showed more variation in their pI. Levels of one Hsp70 isoform each were higher at 24°C and 28°C, and two at 32°C relative to controls. One more basic isoform (spot 112) was lower at 32°C (relative to 24°C). Three more acidic isoforms (spots 73–75) only increased in *M. trossulus* (but were confirmed in *M. galloprovincialis*), all showing an onset temperature (T_{on}) of increased abundance at 32°C.

We identified four sHsp isoforms with masses around 35 kDa in *M. galloprovincialis*. One each had a T_{on} of 24°C and 28°C; the other two had one of 32°C (Fig. 5). In *M. trossulus* we identified four sHsp isoforms, three of which showed higher levels at 28°C and one at 32°C (Fig. 5). One identification has a questionable homology due to a higher molecular mass (spot 95). Of the other three, two highly expressed isoforms overlap with isoforms in *M. galloprovincialis* and show lower T_{on}s in *M. trossulus* [32°C *versus* 28°C; spots 49, 52 (*M. galloprovincialis*) *versus* spots 88, 89 (*M. trossulus*), respectively; Fig. 5]. Thus, in a direct comparison, T_{on}s are lower in *M. trossulus* (but the T_{on}s of other sHsp spots that are not overlapping are similar between the congeners).

In addition, there was a wide range of variation between species in the types of molecular chaperones that showed increased abundance

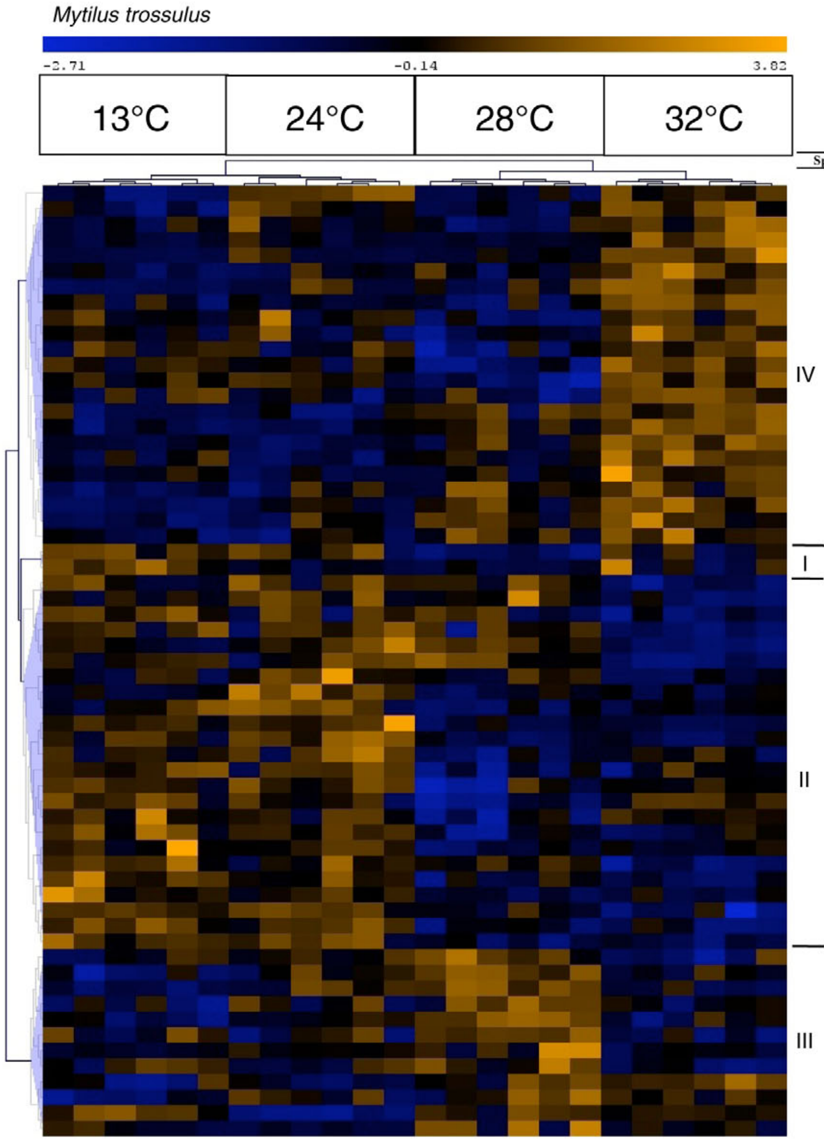

Spot ID	Protein ID	Functional Category
97	Proteasome β-type 4	protein degradation
92	Proteasome α-type 3	protein degradation
83	Proteasome α-type 1	protein degradation
87	α-crystalline-Hsp23	molecular chaperones
61	Tropomyosin	cytoskeletal
43	Hsp70	molecular chaperones
45	Hsp70	molecular chaperones
18	Dihydropteridine reductase	energy metabolism
68	Rho-GDI	signaling
9	Isocitrate dehydrogenase (NADP)	energy metabolism
101	Aspartate amino transferase	energy metabolism
69	Cytochrome c reductase (Rieske center)	energy metabolism
98	Proteasome β-type 4	protein degradation
79	Intermediate filament	cytoskeletal
77	Hsp60	molecular chaperones
76	α-Tubulin	cytoskeletal
73	Hsp70	molecular chaperones
74	Hsp70	molecular chaperones
75	Hsp70	molecular chaperones
118	Hsp70	molecular chaperones
89	α-crystalline-Hsp23	molecular chaperones
88	α-crystalline-Hsp23	molecular chaperones
50	Phenylalanine tRNA sythetase	oxidative stress
22	Isocitrate dehydrogenase (NADP)	energy metabolism
111	Phenylalanine tRNA sythetase	oxidative stress
24	Mito. Malate dehydrogenase	energy metabolism
112	Hsp70	molecular chaperones
8	Cytochrome c reductase (Peptidase M16)	proteolysis / energy metabolism
53	α-Tubulin	cytoskeletal
52	Chaperonin (TCP1)	molecular chaperones
80	Thioredoxin	oxidative stress
14	6-Phospho-glucono lactonase	pentose phosphate
44	Protofiliament ribbon protein	cytoskeletal
23	Arginine kinase	energy metabolism
13	Triose phosphate isomerase	pentose phosphate
36	Proteasome α-type 6	protein degradation
20	NAD-dependent deacetylase (Sirtuin-5)	signaling
7	Tektin	cytoskeletal
11	Mitogen-activated protein kinase (Erk2)	signaling
29	CDC42 (Ras-like GTPase)	signaling
10	Alanopine dehydrogenase	energy metabolism
39	Cytochrome c reductase (Peptidase M16)	proteolysis / energy metabolism
62	Translocon associated protein	energy metabolism
34	F-actin cap protein	cytoskeletal
33	Glutamine synthetase	amino acid metabolism
54	Hsp70	molecular chaperones
5	Fascin	cytoskeletal
37	Fascin	cytoskeletal
16	NADH dehydrogenase	energy metabolism
96	Aldehyde dehydrogenase	oxidative stress
95	α-crystalline-Hsp23	molecular chaperones
51	Hsp70	molecular chaperones
113	Dyp-type peroxidase	oxidative stress
66	Proteasome β-type 3	protein degradation
105	Radial spoke head 1 homolog	cytoskeletal
57	Thiamine pyrophosphate transketolase	pentose phosphate
114	Pyruvate dehydrogenase (E1-β)	energy metabolism
21	Citrate synthase	energy metabolism
109	Cyclophilin	molecular chaperones
26	Proteasome β-type 6	protein degradation
31	Galactose-binding lectin	cell adhesion

Fig. 3. Hierarchal clustering of identified proteins using Pearson's correlation in response to acute heat stress in the cold-adapted *Mytilus trossulus*. For further details, see Fig. 2.

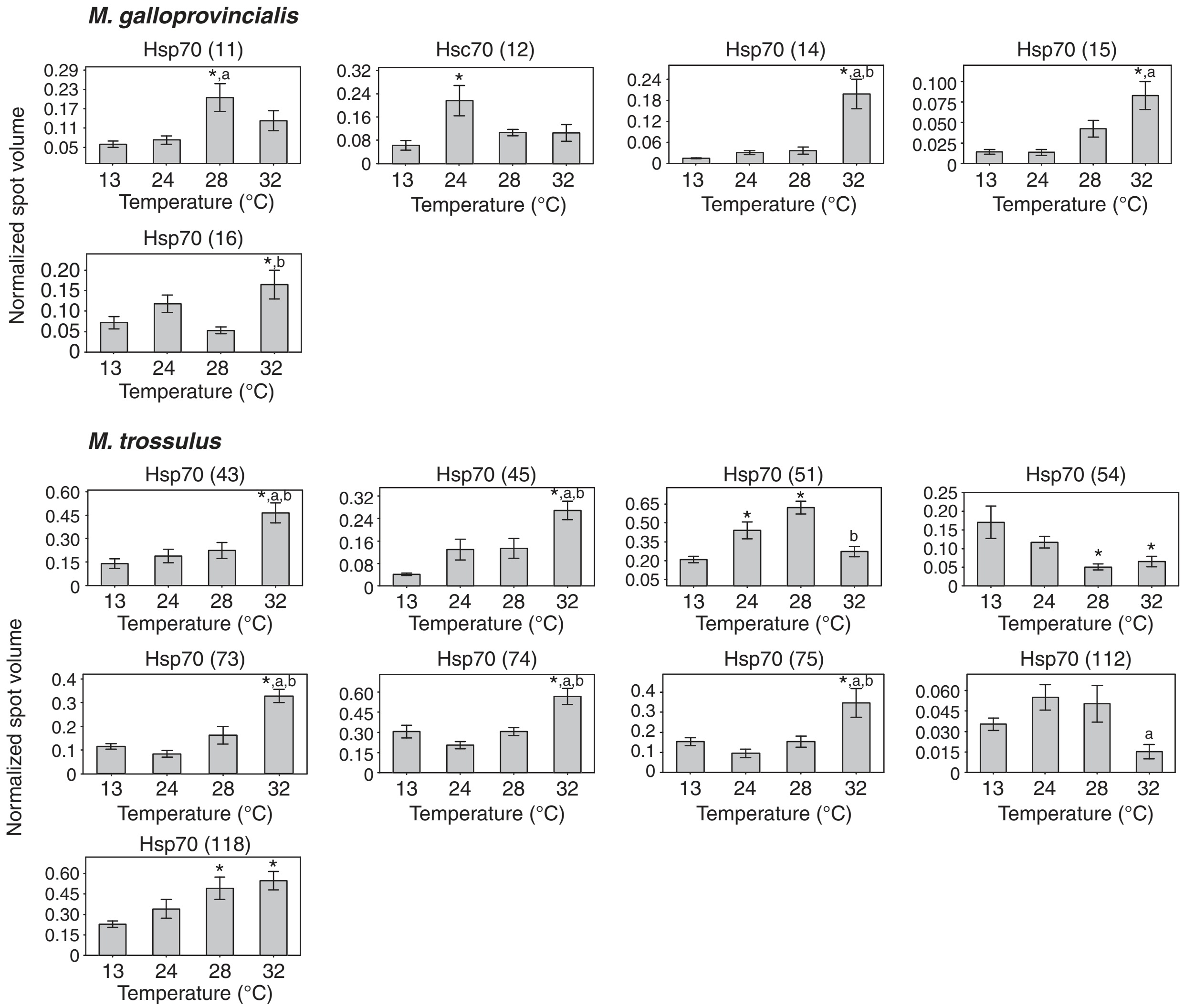

Fig. 4. Levels of molecular chaperones (Hsp70s) in gill tissue of *Mytilus* congeners in response to heat stress (24°C, 28°C and 32°C). Spot volumes were obtained by normalizing against the volume of all proteins and show means ± 1 s.e.m. (N=6). '*' indicates P<0.05 relative to the control (13°C), 'a' relative to 24°C, and 'b' relative to 28°C (Tukey pairwise comparison). Spot numbers are shown in parentheses.

(Hsp90, Hsp70, chaperonin, sHsp and cyclophilin; see Figs 2–5 and supplementary material Tables S1 and S2). In a direct comparison of overlapping and identical spots, *M. trossulus* tended to induce changes in (acidic) Hsp70 (32°C *versus* non-detected change) and sHsp levels (28°C *versus* 32°C) at a lower temperature than the warm-adapted *M. galloprovincialis* (Figs 4 and 5). Expression of sHsp transcripts also differed between the congeners and was statistically the most distinct species-specific characteristic (Lockwood et al., 2010). Broadly speaking, these results generally confirm those of a previous comparison of the heat shock responses of these two species using ^{35}S-labelled amino acids (Hofmann and Somero, 1996a). Importantly, this shows that our quantitative comparison of protein abundance is comparable with other highly sensitive detection methods.

Our study demonstrates the quantitative contribution of sHsps (about 2.5% of total protein at 32°C), which is further evidence for the crucial role these chaperones play in protecting cells from acute heat stress and in indicating interspecific differences in thermal tolerance (Norris and Hightower, 2002; Sanders et al., 1991; Tomanek, 2005; Tomanek, 2010; Tomanek and Somero, 1999). Upon heat shock, sHsps are activated by a change in their oligomerization state and through phosphorylation; subsequently, they bind to denaturing proteins and prevent their aggregation (Haslbeck et al., 2005). However, proteins that are stabilized by sHsps during stress require the activity of ATP-dependent Hsps, e.g. Hsp70, to refold correctly. Small Hsps play multiple roles during acute heat stress. They play an especially important role in stabilizing cytoskeletal elements (actin microfilaments, intermediate filaments and microtubules); they exert an anti-apoptotic activity and, additionally, enhance the cell's ability to combat oxidative stress (Arrigo, 2007; Concannon et al., 2003). Although there is still uncertainty about the causality *versus* correlation of these events, sHsps are key players in the coordinated effort of protecting the cell from the simultaneous stress of heat and reactive oxygen species (ROS).

Protein degradation

The central role that thermal and oxidative damage to proteins plays in heat stress is further manifested by the observed changes in the levels of proteins involved in proteolysis, including proteins that form the major protein-degrading structure of the cell, the proteasome (Glickman and Ciechanover, 2002). Four of the five proteasome isoforms identified in *M. galloprovincialis* showed

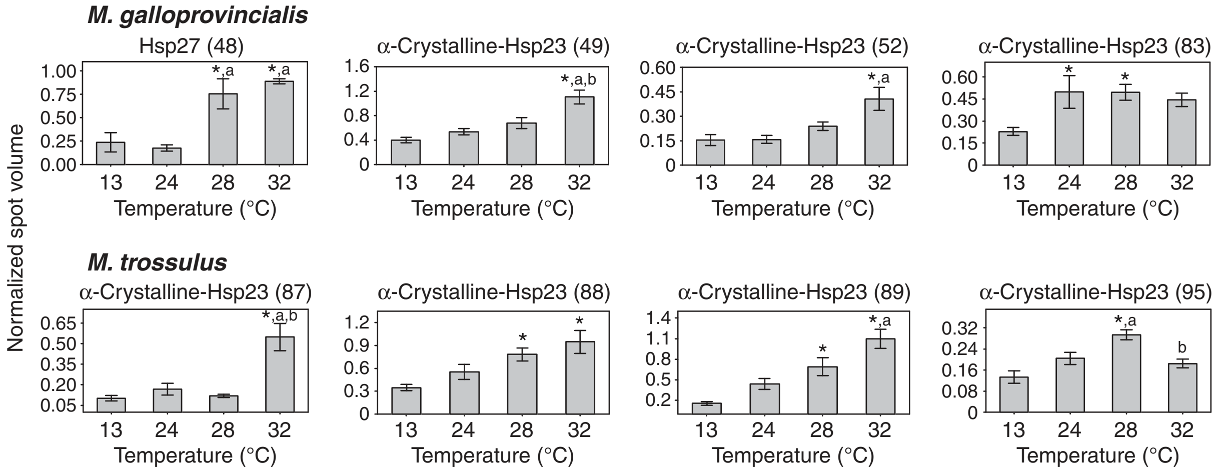

Fig. 5. Levels of molecular chaperones (small Hsps) in gill tissue of *Mytilus* congeners in response to heat stress (24°C, 28°C and 32°C). For further details, see Fig. 4 legend.

significantly lower levels with heat stress, starting at 24°C, 28°C or 32°C (Figs 2 and 6). In three of these subunits there was a direct overlap of spot positions and identities with *M. trossulus* [Fig. 1; spots 45, 51, 53 (*M. galloprovincialis*) *versus* spots 83, 66, 36 (*M. trossulus*), respectively], and all three subunits showed significantly higher levels with heat stress in *M. trossulus* (Fig. 6). Two other subunits (spots 92 and 97), which we only identified in *M. trossulus*, also showed greater abundance with heat stress. Two additional isoforms (spots 26 and 98) showed lesser abundance at 24°C and 28°C (relative to the control), respectively, but increased abundance at 32°C relative to 24°C and 28°C, respectively.

The interspecific differences in the levels of proteasomal subunits in response to heat stress in our proteomic study and in the parallel transcriptomic analysis (Lockwood et al., 2010) – primarily lower levels in *M. galloprovincialis* and higher levels in *M. trossulus* – need to be interpreted in the context of up-stream production of proteasomal substrates. Levels of ubiquitin conjugates, which are proteins tagged for degradation by the proteasome, increase in response to heat stress in *Mytilus* (Hofmann and Somero, 1996b), suggesting that a greater number of proteasome building blocks may be required for processing the conjugates in heat-stressed specimens. Inherent interspecific differences between the congeners may exist, because ubiquitin conjugate levels were lower in *M. galloprovincialis* than in *M. trossulus* following acclimation to 13°C for several weeks (Hofmann and Somero, 1996a). Thus, the increased levels of proteasomal subunits observed only for *M. trossulus* in the present study and the transcriptomic analysis (Lockwood et al., 2010) could reflect a response to increased levels of ubiquitin conjugates.

Alternatively, the lower levels of proteasome subunits in *M. galloprovincialis* may be a strategy to temporarily reduce ATP consumption by the proteasome, thus providing energy for the higher ATP-consuming chaperoning activity by Hsp70 and other molecular chaperones. A third explanation considers the extent to which protein degradation and translation control protein abundance during heat shock. Severe heat shock is characterized by an arrest of translation of proteins other than molecular chaperones, in part to avoid exposing nascent polypeptide chains to denaturing conditions (Holcik and Sonenberg, 2005). Under such conditions, lowering the rate of protein degradation could be an alternative means of maintaining or increasing protein abundance by prolonging the lifespan of a protein. Evidence for such a scenario was recently described when the effects of low and high levels of inhibition of proteasomal activity on the proteome were compared in human endothelial cells (Bieler et al., 2009). Low inhibition led to the induction of a protective oxidative stress response by specifically prolonging the lifespan of oxidative stress proteins. Thus, the down-regulation of proteasome subunits in *M. galloprovincialis* could compensate for the lower rates of protein synthesis indirectly by slowing the degradation of oxidative stress proteins, thereby increasing the cell's ability to respond to oxidative stress. Whichever one of these explanations may be correct, our results suggest that the regulation of protein degradation contributes to determining the variation in the cellular stress response that underlie interspecific differences in thermal tolerance.

Anaerobic energy metabolism

Under conditions of high ATP demand and inadequate aerobic production of ATP, cells can quickly, but only for a limited time, replenish ATP by transferring phosphoryl groups from other high-energy nucleotide bonds, e.g. phosphoarginine or GTP (Ellington, 2001). Levels of several proteins involved in the transfer of phosphoryl or pyrophosphoryl groups from or to ATP either for biosynthesis (pyrophosphatase) or for the formation of nucleoside triphosphates (nucleoside diphosphate kinase; see Aerobic energy metabolism for a discussion) and phosphoarginine (arginine kinase) were lower in *M. galloprovincialis* at 28°C or 32°C (Figs 2 and 7). Levels of arginine kinase were also lower in *M. trossulus* at 28°C and 32°C relative to 24°C (Figs 3 and 7). Arginine kinase has been proposed to increase the ability of invertebrates to cope with the stress of variable environmental conditions related to hypoxia and acidosis (Ellington, 1989; Ellington, 2001). Recent transcriptomic and proteomic studies have shown that arginine kinase changes in response to temperature stress, but with inconsistent responses among species (Gracey et al., 2008; Martinez-Fernandez et al., 2008; Teranishi and Stillman, 2007). We interpret the decrease in arginine kinase in our study as an indication of the metabolic depression that is known to occur during the emersion of intertidal mussels, which often coincides with thermal stress (Shick et al., 1988). This is despite the fact that our animals were immersed and thus theoretically able to take up oxygen while they experienced heat stress.

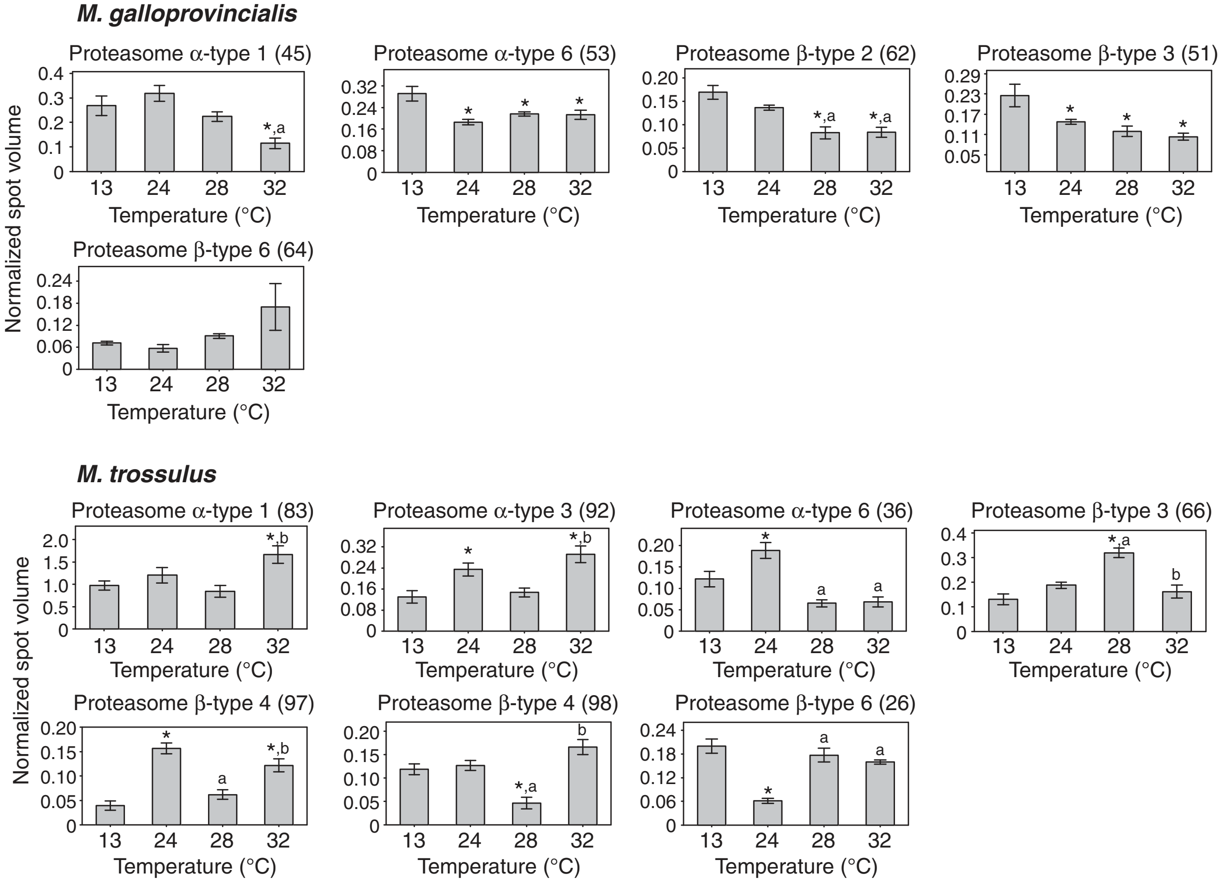

Fig. 6. Levels of proteasome isoforms in gill tissue of *Mytilus* congeners in response to heat stress (24°C, 28°C and 32°C). For further details, see Fig. 4 legend.

Levels of three enzymes, i.e. phosphoenolpyruvate carboxykinase (PEPCK, which also plays an important role in gluconeogenesis), aspartate aminotransferase (AAT) and the cytosolic isoform of malate dehydrogenase (cMDH), which are connected through direct metabolic reactions and are active in mollusks during anaerobiosis, were lower at 24°C (PEPCK) and 32°C (AAT and cMDH) in *M. galloprovincialis* (Figs 2 and 7). In *M. trossulus* alanopine dehydrogenase, another enzyme known to be active under anaerobic conditions, showed lower levels at 28°C. By contrast, levels of AAT were higher at 32°C in comparison with 28°C in *M. trossulus*.

The three reactions linking PEPCK, AAT and cMDH constitute an alternative anaerobic pathway in marine invertebrates (Hochachka and Somero, 2002; Zwaan and Mathieu, 1992). We hypothesize that the decrease observed for these three proteins in *M. galloprovincialis* at one of the treatment temperatures is further evidence for a decrease in metabolism in response to heat stress and overrides any increased requirement for the anaerobic production of ATP. Alternatively, the lower abundance of AAT and cMDH may indicate that the shuttling of reducing equivalents (NADH) from the cytosol to the mitochondria through the malate–aspartate shuttle is reduced in *M. galloprovincialis* at the highest temperature (Salway, 2004). In *M. trossulus* alanopine dehydrogenase, which converts pyruvate into alanopine while oxidizing NADH to NAD^+, also showed a heat-induced decrease in abundance while AAT increased from 28°C to 32°C. This suggests that while some alternative anaerobic pathways may be down-regulated in *M. trossulus* in response to heat stress others are up-regulated to feed specific metabolic pathways (see below).

Aerobic energy metabolism

Under aerobic conditions ATP production is mainly driven by the supply of NADH, which is produced by glycolysis and reactions in the Krebs cycle (Hochachka and Somero, 2002). NADH is oxidized at the beginning of the electron transport chain (ETC) where the generation of a proton gradient fuels ATP synthesis (Fig. 11). In the case of *M. galloprovincialis* the only enzyme changing abundance representing these pathways were three isoforms of NADP-dependent isocitrate dehydrogenase (IDH). Two of those IDH isoforms decreased with heat stress (24°C to 32°C) while another one increased (24°C to 32°C) relative to the control (Fig. 7).

By contrast, in *M. trossulus* six enzymes of these core metabolic pathways changed abundance in response to heat stress. Four of those enzymes belong to the Krebs cycle or linking glycolysis to it. Pyruvate dehydrogenase (PDH), a key regulatory enzyme determining the flux through the cycle, and mitochondrial malate dehydrogenase (mMDH) were down at 32°C relative to 28°C (Fig. 7). By contrast, levels of citrate synthase were up at 32°C relative to the control. One isoform of IDH showed a decrease from the control and 24°C to 28°C and another one showed an increase in abundance from 28°C to 32°C (Figs 2 and 7).

Two additional metabolism-related enzymes that changed abundance in *M. trossulus* are part of the ETC. The ETC is the major source of ROS, such as superoxide anions ($^{\bullet}O_2^-$), hydrogen

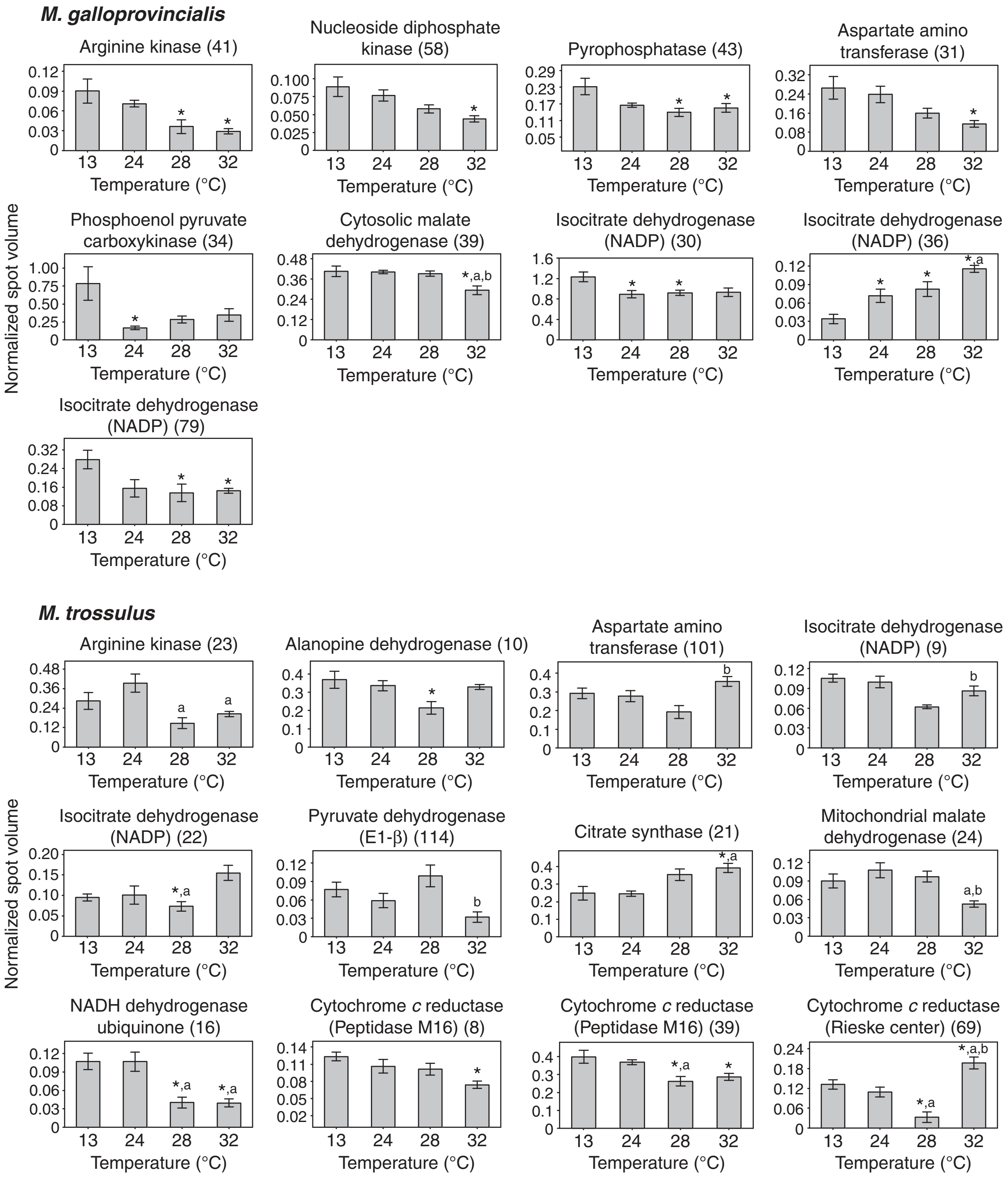

Fig. 7. Levels of proteins implicated in energy metabolism in gill tissue of *Mytilus* congeners in response to heat stress (24°C, 28°C and 32°C). For further details, see Fig. 4 legend.

peroxides (H_2O_2) and hydroxyl radicals ($^{\bullet}OH$) (Fig. 11) (Chandel and Schumacker, 2000; Murphy, 2009). Temperature stress has been shown to increase the production of ROS in mitochondria, simply due to a Q_{10}-effect that will approximately double the speed of the electron flux through the ETC with every 10°C increase in temperature (Abele et al., 2002). NADH dehydrogenase (also called NADH:ubiquinone oxidoreductase), complex I of the ETC, oxidizes NADH to NAD^+. Its abundance was lower at 28°C and 32°C in *M. trossulus* (Figs 2 and 7). Reducing the entry of NADH into the ETC by decreasing the expression of NADH dehydrogenase could ameliorate an increase in ROS production (Fig. 11). Another multiple subunit ETC enzyme, cytochrome *c* reductase (also called the cytochrome *bc* complex or complex III), showed mixed changes in *M. trossulus* only; levels of two subunits that show sequence homology with the mitochondrial processing peptidase M16 and that are similar to the core protein of cytochrome *c* reductase (Braun and Schmitz, 1995) were down at 28°C (spot 39) and 32°C (spots 8 and 39) relative to the control, but the subunit that contains the

Rieske iron–sulfur center first decreased at 28°C and then increased at 32°C relative to the control in *M. trossulus*. These results may be an indication of a down-regulation of the ETC and thus ROS production at 32°C; a scenario that is further supported by a reduced flux through the Krebs cycle and thus the decreased production of NADH, catalyzed by the lower levels of PDH at 32°C relative to 28°C and mMDH at 32°C relative to 24°C and 28°C (Figs 7 and 11). The related study on the gene expression of *Mytilus* congeners (Lockwood et al., 2010) showed the opposite trend for NADH dehydrogenase and PDH, indicating that translational or post-translational regulation may play an important role in changing the abundance of these proteins.

Although the down-regulation of nucleoside diphosphate kinase in *M. galloprovincialis* could possibly indicate a similar slowdown of the Krebs cycle, mainly because the enzyme converts the GTP that is formed by the succinyl CoA synthetase reaction in the mitochondrial matrix into ATP (Salway, 2004), broader changes indicating reduced NADH production are only observed in *M. trossulus* at 32°C (Fig. 11).

NADPH, in contrast to NADH, is used as reducing equivalent (by glutathione reductase) to reduce glutathione, a major cellular antioxidant that helps scavenge ROS under oxidative stress. Thus, it is possible that a cell under heat stress will undergo a shift from a temperature-induced NADH-fueled increase in ETC activity that leads to increased ROS production to the production of NADPH to defend itself against increasing levels of macromolecular damage by ROS (Fig. 11). Depending on the isoform, IDH can catalyze the oxidation of isocitrate with either NAD^+ or $NADP^+$ as an electron acceptor, producing the reduced form (Jo et al., 2001). The isoforms we identified are of the NADP-dependent type, so possibly the increasing levels of some of the different IDH isoforms indicate an increase in NADPH production (Jo et al., 2001); a conclusion that is further supported by the expression of proteins of the pentose phosphate pathway (see below). Thus, we present support for the hypothesis (see below) that *Mytilus* gill tissue may decrease the production of NADH but increase its production of NADPH in response to heat stress. To increase NADPH production it is necessary to feed the reaction of IDH and maintain or even increase the abundance of citrate synthase, using oxaloacetate as a substrate that is possibly provided by increasing levels of AAT (Fig. 11); AAT increased abundance at 32°C (relative to 28°C) in *M. trossulus* but decreased at 32°C (relative to the control) in *M. galloprovincialis* (Fig. 7). For this scenario to occur despite the reduced expression of PDH, acetyl CoA, required by citrate synthase, may come from the catabolism of branched-chain amino acids (isoleucine, valine, leucine), lysine, tryptophan or fatty acids (Salway, 2004).

Oxidative stress proteins

Several of the enzymes that changed in abundance are known to respond to an increase in oxidative stress (Figs 2, 3 and 8). Two closely localized superoxide dismutase (SOD) isoforms (Fig. 1; spots 72 and 73) reversed abundance in *M. galloprovincialis*: one isoform decreased at 28°C and 32°C while the other increased, suggesting a PTM (Fig. 8). Levels of two different enzymes, thioredoxin and aldehyde dehydrogenase, were lower at 32°C (relative to the control, 24°C and 28°C, respectively) in *M. trossulus* (Fig. 8).

SOD, thioredoxin and aldehyde dehydrogenase are all part of the minimal stress proteome of cellular organisms (Kültz, 2005) and are implicated, along with IDH, in the regulation of the cell's redox balance. They either reduce ROS (SOD), thiol groups (thioredoxin) or aldehydes (aldehyde dehydrogenase) that form due to oxidative stress or produce NADPH to replenish diminishing levels of reducing equivalents (IDH; Fig. 11). In *M. galloprovincialis* one IDH and one SOD isoform increased at 24°C and 28°C, respectively (Figs 7 and 8). By contrast, in *M. trossulus* the abundance of two of these enzymes (thioredoxin and aldehyde dehydrogenase) decreased at 32°C, suggesting that this may be a temperature to which it cannot adequately respond, and thus indicating that the two species differ in their cellular response to oxidative stress (also see pentose–phosphate pathway).

Levels of NADP-dependent dihydropteridine reductase were higher in *M. trossulus* at 32°C relative to 13°C, 24°C and 28°C (Figs 3 and 8). It is required for the synthesis of tetrahydrobiopterin, a cofactor for enzymes involved in the catabolism of aromatic amino acids, e.g. phenylalanine (Salway, 2004). Tetrahydropteridine has been proposed to act as a reducing agent similar to reduced glutathione (Ponzone et al., 2004). Dyp-type peroxidase catalyzes the reaction from H_2O_2 to H_2O and a ($^{\bullet}OH$) radical, similar to the one of catalase (Sugano, 2009). Its abundance was found to be greater in *M. trossulus* at 28°C (Figs 3 and 8).

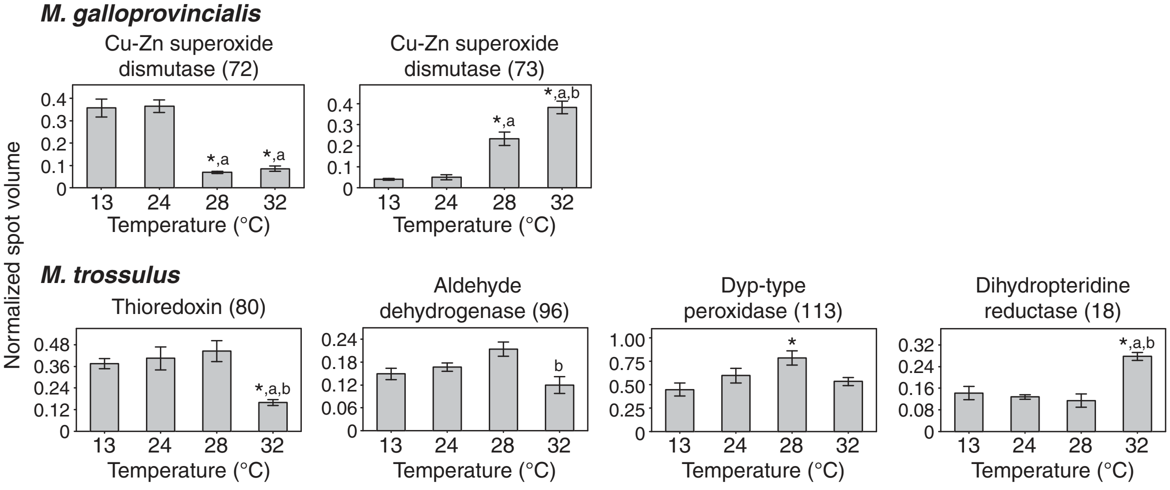

Fig. 8. Levels of proteins implicated in oxidative stress in gill tissue of *Mytilus* congeners in response to heat stress (24°C, 28°C and 32°C). For further details, see Fig. 4 legend.

The expression profiles of putative oxidative stress proteins indicate that the warm-adapted *M. galloprovincialis* has the ability to cope with heat-induced oxidative stress over the upper range of temperatures experienced in our experiment while the response of the cold-adapted *M. trossulus* seems to be limited to a temperature of up to 28°C.

Pentose–phosphate pathway

The pentose–phosphate pathway normally diverts glucose from glycolysis to produce pentose (ribose-5-phosphate) to make RNA, DNA and several coenzymes (Fig. 11). Alternatively, the pentose can be recycled into glucose 6-phosphate *via* a non-oxidative phase that is dependent on a thiamine pyrophosphate transketolase (Nelson and Cox, 2008). This leads to the production of reducing equivalents (NADPH) that are used to replenish oxidized glutathione, which is required to counter the damaging effects of ROS on macromolecules (Go and Jones, 2008). The expression of two enzymes of the pentose–phosphate pathway was affected by heat stress. Levels of 6-phosphoglucono-lactonase were higher at 32°C in *M. galloprovincialis* (Fig. 9). Levels of this enzyme were down at 28°C and 32°C relative to 24°C in *M. trossulus*. Thiamine pyrophosphate transketolase showed increased levels at 24°C or 28°C in the former and the latter species, respectively (Fig. 9). In *M. trossulus*, levels of thiamine pyrophosphate transketolase decreased from 28°C to 32°C.

At this point it is unclear if the interspecific differences in the pentose–phosphate pathway have any relevance for the variation in thermal tolerance. However, the identification of at least two enzymes of this pathway, in conjunction with the identification of SOD, an enzyme closely linked to the increase of ROS, in *M. galloprovincialis* and the contribution of these enzymes (lactonase and thiamine pyrophosphate transketolase) to the second components of the PCAs conducted for both species (see below) provide further evidence for the important role of ROS under conditions of heat stress.

Cytoskeletal proteins

Several actins and tubulins as well as actin- and tubulin-binding proteins changed abundance in response to heat stress (Figs 2 and 3). We identified nine (α and β) tubulin isoforms as changing abundance in *M. galloprovincialis*. In seven of the eight, levels initially increased at either 24°C (three isoforms) or 28°C (four isoforms) and then decreased at 32°C (mostly cluster III; Fig. 2). Cluster III also includes Hsp90. By contrast, in *M. trossulus* the same cluster includes three chaperones, two proteasome subunits, three oxidative stress proteins and two proteins involved in energy metabolism but no tubulin and only one other cytoskeletal protein (Fig. 3). We also identified two actin isoforms in *M galloprovincialis*, which showed an increase from lower (24°C and 28°C) to higher (32°C) temperatures. Several cytoskeletal proteins elevated and maintained high levels in *M. trossulus* at 28°C (α-tubulin) or 32°C (α-tubulin, intermediate filament and tropomyosin).

Gelsolin, an actin-binding protein and a regulator of actin filament assembly, decreased from 24°C to 32°C in *M. galloprovincialis* (Fig. 2). Two isoforms of the actin-bundling fascin, the tubulin-binding tektin, protofilament ribbon protein, radial spoke protein and an F-actin capping protein decreased at either 28°C or 32°C in *M. trossulus* (Adams, 2004; Hinchcliffe and Linck, 1998; Setter et al., 2006). They are all part of clusters II and III (Fig. 3) that include proteins whose abundances generally decreased in response to heat stress (at 28°C and 32°C). None of these proteins were identified for *M. galloprovincialis*.

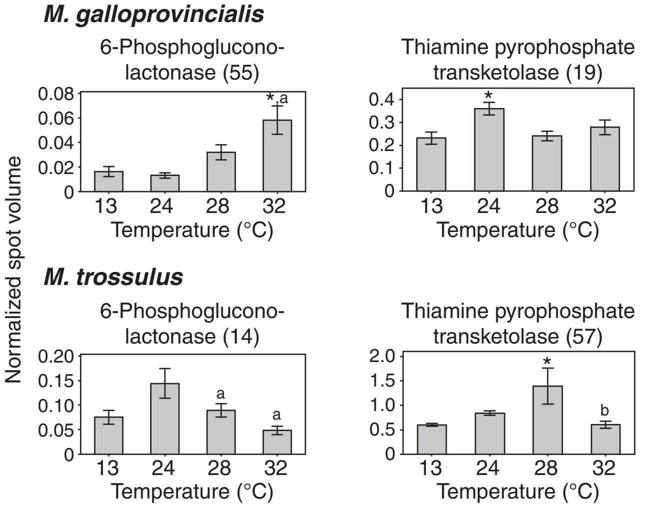

Fig. 9. Levels of proteins implicated in the pentose–phosphate pathway in gill tissue of *Mytilus* congeners in response to heat stress (24°C, 28°C and 32°C). For further details, see Fig. 4 legend.

In the warm-adapted *M. galloprovincialis* there is a general trend of tubulin levels being higher at 24°C and 28°C then lower at 32°C, i.e. the temperature at which sHsps that are implicated in binding and stabilizing cytoskeletal protein components show greater abundance. It is surprising that we only identified two tubulin isoforms in the cold-adapted *M. trossulus* and no actin isoforms that changed abundance even though a number of actin-binding proteins were down at 28°C and 32°C while sHsps were up. PCAs of the protein expression patterns of these two congeners confirm the importance of tubulin for explaining interspecific differences in their heat shock responses (see below). These interspecific differences among cytoskeletal proteins in response to heat shock are important because they may, in part, be the underlying reason for the differences in the expression of molecular chaperones, specifically the sHsps.

Signaling proteins

The specific functions of signaling proteins in the response of cells to environmental stress are often complex due to the networks of interacting signaling cascades (Marks et al., 2009). These cascades are often activated by PTMs, e.g. phosphorylation, that can result in a shift in the pI of the protein. However, such changes may be only affecting a small fraction of already relatively low-abundance proteins, which makes these PTMs difficult to detect with our approach.

We identified several signaling proteins that changed in abundance in one or the other species (Figs 2, 3 and 10): Levels of the Ras-like GTPase RhoA showed elevated levels at 28°C and 32°C in *M. galloprovincialis*. Another Ras-like GTPase (cdc42) and a mitogen-activated kinase (Erk2) were lower at 28°C but not at 32°C in *M. trossulus*. RhoA and cdc42 are both members of the Rho (Ras-like) family of small G-proteins that affect cell shape and motility by controlling the dynamics of the actin cytoskeleton (Burridge and Wennerberg, 2004; Marks et al., 2009). RhoA is activated by hypoxia due to an increase in ROS in mammalian endothelial cells (Dada et al., 2007) and is a key regulator in the formation of actomyosin stress fibers (Burridge and Wennerberg, 2004). Although cdc42 is implicated in directly activating the JNK (c-Jun N-terminal kinase) and p38 mitogen-activated protein kinase (MAPK) pathways

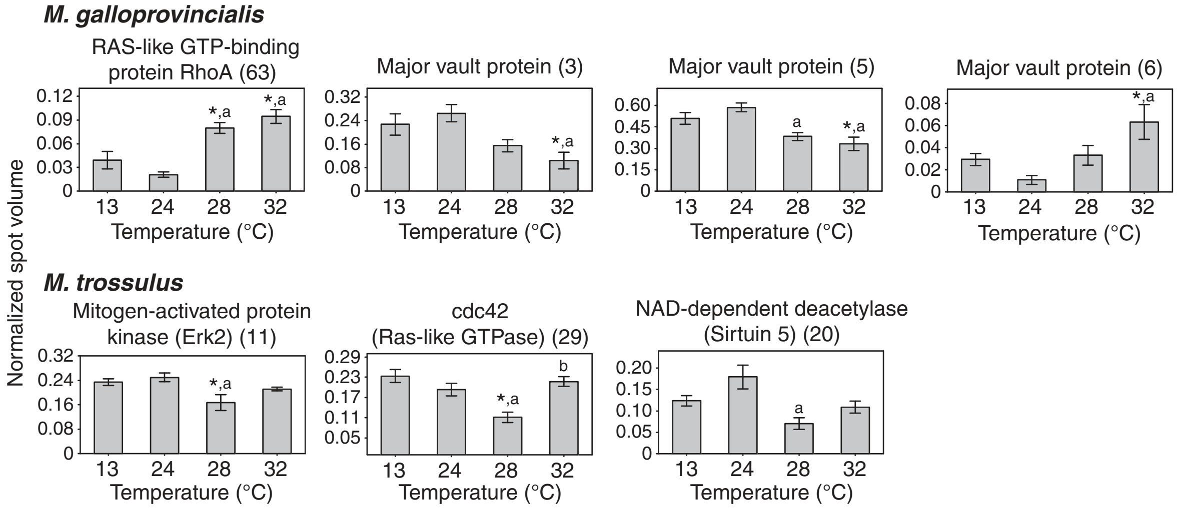

Fig. 10. Levels of proteins implicated in cellular signaling processes in gill tissue of *Mytilus* congeners in response to heat stress (24°C, 28°C and 32°C). For further details, see Fig. 4 legend.

(Cowan and Storey, 2003), it has also been shown that it forms a complex with MAPK/Erk *via* the interaction domains of IQGAP1 (IQ motif containing GTPase-activating protein), which subsequently leads to the association of the complex with F-actin (Bourguignon et al., 2005; Kolch, 2005).

A prominent row of up to eight protein isoforms around 100 kDa can be seen to exist in both congeners (Fig. 1). We identified two of those as the major vault protein (MVP). These isoforms showed decreased levels at 32°C in *M. galloprovincialis* but not in *M. trossulus* (Fig. 10, data not shown for *M. trossulus*). A third MVP, an acidic isoform (spot 6), showed increased abundance at 32°C only in *M. galloprovincialis*. MVPs are part of the ubiquitous vault particles, barrel-shaped cellular structures that exceed the size of ribosomes (Suprenant et al., 2007). Despite 20 years of research, the exact function of MVP is still unclear. Vault complexes are implicated in the cellular response to environmental toxins (Berger et al., 2009). They also bind to several effectors of signaling cascades that are stress induced, such as the pro-apoptotic phospholipid phosphatase PTEN (phosphatase and tensin homolog) pathway, an antagonist of the phosphatidylinositol 3-kinase, and the epidermal growth factor (EGFR)-induced MAPK pathway (Berger et al., 2009). A survey of stressors affecting the transcription of MVP in *M. edulis* showed the gene to be responsive to anaerobic conditions but not to changes in osmolality or temperature (Luedeking and Koehler, 2004). The relevance of the species-specific response to temperature that we observed is unclear. The lowering of levels of the two relatively abundant MVP isoforms in *M. galloprovincialis* could be part of an anti-apoptotic response. Given that these proteins constitute more than 2% of the protein abundance in our gels, elucidating their exact role seems important to completely understand the cellular response to stressful conditions.

Hypotheses integrating the observed heat-stress-induced changes in the proteome

To integrate the observations discussed above, we state three testable hypotheses that provide an interpretative framework for the heat-stress-induced changes observed in the proteomes of the two congeners.

Hypothesis 1: sHsps stabilize cytoskeletal proteins in response to oxidative and heat stress

Changes in the abundance of multiple cytoskeletal proteins, including tubulin, actin and intermediate filament, occur during heat stress in both species. Of all of the proteins that we identified, 26% and 16% in *M. galloprovincialis* and *M. trossulus*, respectively, are part of the cytoskeleton. In addition, increasing levels of the signaling protein Rho A, a small G-protein, in *M. galloprovincialis* suggest that gill cells are undergoing complex changes of their cytoskeleton during heat stress, possibly leading to the formation of actomyosin stress fibers and focal adhesions (Burridge and Wennerberg, 2004; Marks et al., 2009). The changes may be triggered through heat-induced changes in the stability of the cytoskeleton and thus may indicate that cytoskeletal proteins are the ‘weak’ elements during heat stress that trigger the expression of molecular chaperones such as sHsp (Arrigo, 2007), chaperonins (TCP-1) and Hsp70s (Liang and MacRae, 1997). However, heat-induced ROS may be important co-stressors that are also affecting the stability or dynamics of the cytoskeleton. There is strong evidence for the role of ROS in inducing a number of cytoskeletal rearrangements (Dalle-Donne et al., 2001; Huot et al., 1997; Huot et al., 1998), specifically triggering an increase of tubulin and actin (Clarkson et al., 2002). The increase in a number of tubulin isoforms in *M. galloprovincialis* at 24°C and 28°C and the subsequent decrease at 32°C (Fig. 2, cluster III) illustrates a similar response. Although their importance in contributing to the heat shock response is recognized, the nature and functional relevance of cytoskeletal changes in response to heat and oxidative stress is still poorly understood (Dalle-Donne et al., 2001; Tell, 2006).

Increased synthesis of sHsp (Figs 2 and 3) can be triggered through the ROS-mediated denaturation of cytoskeletal proteins (Arrigo, 2007; Huot et al., 1996; Lavoie et al., 1995). Upon heat shock, sHsps bind and stabilize cytoskeletal elements, exert anti-apoptotic activity and modulate the oxidative and heat stress response, suggesting that sHsps can stabilize cytoskeletal proteins under both conditions (Concannon et al., 2003). There is also evidence for the role of ROS in directly regulating the activity of Hsps, in particular sHsps, through the oxidation of cysteine residues (Diaz-Latoud et al., 2005; Jakob et al., 1999). In turn, overexpression

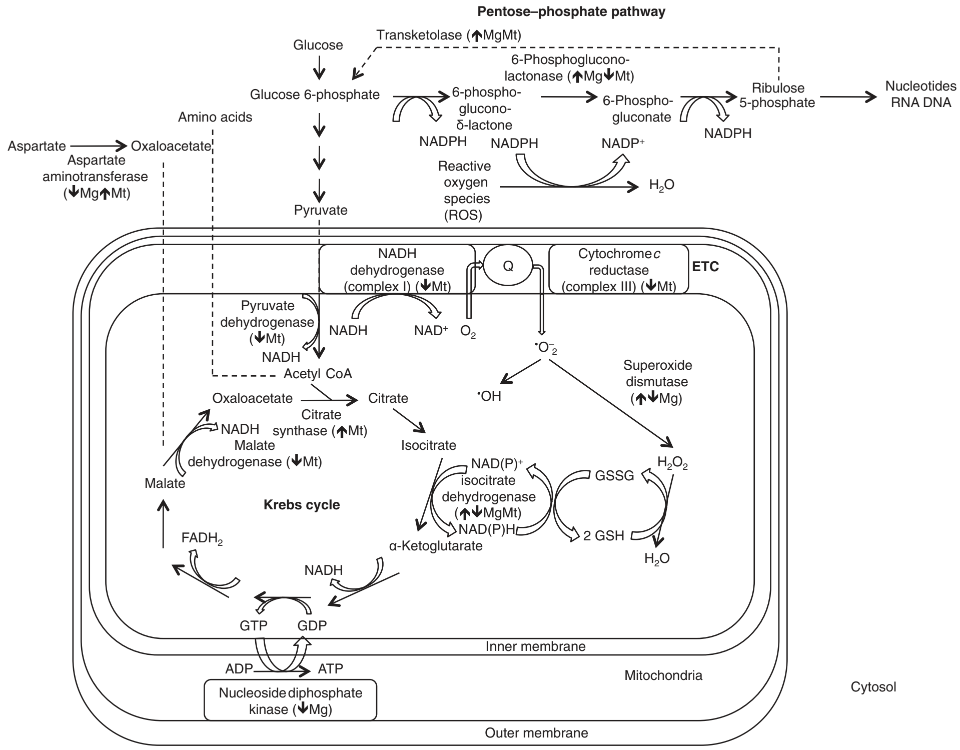

Fig. 11. Metabolic reactions involved in the putative switch from NADH- to NADPH-producing pathways. Proteins that changed abundance in response to heat stress are shown in italics (‘↑’ denotes an increase, ‘↓’ denotes a decrease and ‘↑↓’ denotes an increase and a decrease in the abundance of protein isoforms depending on treatment). Species-specific changes are indicated as *Mg* (*Mytilus galloprovincialis*) or *Mt* (*Mytilus trossulus*). ETC (electron transport chain). Abbreviations that are not used in the main text are: glutathione, and its oxidized form (GSH, GSSG), ubiquinone (Q). For details, see main text.

of sHsps has been shown to attenuate oxidative stress-induced apoptosis in mouse fibroblast cells (Lee et al., 2004).

In summary, our data provide further support for the hypothesis that there are close links between cytoskeletal modifications caused directly by heat or through heat-induced oxidative stress and the increased expression of sHsps.

Hypothesis 2: sirtuin – a possible regulator of metabolic changes in response to heat stress

One enzyme that has not yet been discussed but that changed levels in *M. trossulus* is an NAD-dependent deacetylase, sirtuin 5. Its abundance decreased significantly from 24°C to 28°C (Figs 3 and 10).

Sirtuins are up-regulated in response to caloric restriction, and overexpression has been shown to extend lifespan in such diverse organisms as yeast, worms and fruit flies (Finkel et al., 2009; Schwer and Verdin, 2008). Deacetylation by sirtuins can increase the activity of some proteins but inhibit the activity of others (Ahn et al., 2008; North and Sinclair, 2007; Schlicker et al., 2008). The deacetylation activity of sirtuins is controlled by the cellular NADH:NAD$^+$ ratio and thus the redox status of the cell (Lin et al., 2004). Protein acetylation in general has been shown to control wide-ranging metabolic changes (Wang et al., 2010; Zhao et al., 2010). Metabolic processes that have been shown to be regulated by the deacetylation activity of sirtuins include fatty acid metabolism, gluconeogensis and Krebs cycle activity (North and Sinclair, 2007) as well as the ETC (Ahn et al., 2008). Specifically, deacetylation regulates the activity of IDH (Schlicker et al., 2008), cytochrome *c* reductase (Ahn et al., 2008) and MDH (Zhao et al., 2010); three enzymes we identified in *M. trossulus* together with sirtuin 5. A recent study identified a number of proteins interacting with sirtuins (Law et al., 2009), including several Hsp70s and MAPK/Erk; again, these are proteins we found responding to acute heat stress in *Mytilus*. In addition, a reduction in MAPK/Erk is generally associated with reduced cell survival (Nadeau and Landry, 2007), an observation consistent with our results in *M. trossulus* and the reduction of the sirtuin 5 isoform (Figs 3 and 10). Importantly, it has been shown that sirtuins interact with and regulate the DNA-binding activity of heat-shock factor 1 and that down-regulation of sirtuin 1 leads to the attenuation of the heat shock response (Westerheide et al., 2009).

Given the known interactions between sirtuins and at least five proteins that we found to respond to heat stress (either by changing abundance or through PTMs), we hypothesize that sirtuins are regulators of the metabolic costs of heat stress, indicated by the reduced protein levels of sirtuins in *Mytilus*. Furthermore, this suggests that the acetylation status of proteins is a key PTM that warrants more attention in the study of how heat stress affects cellular metabolism (Choudhary et al., 2009; Westerheide et al., 2009; Zhao et al., 2010).

Hypothesis 3: heat shock causes a switch from NADH- to NADPH-producing metabolic pathways

An increase in temperature by 15°C will almost triple reaction rates and thus the flux through the ETC, increasing the production of ROS. Increasing flux through the ETC is fueled by NADH. By contrast, NADPH is necessary to neutralize ROS, mainly by reducing glutathione (by glutathione reductase), which in turn reduces ROS through the glutathione peroxidase reaction (Go and Jones, 2008) (Fig. 11). Changes in both the pentose–phosphate pathway and NADP$^+$-dependent mitochondrial IDH suggest that there is an up-regulation in the production of NADPH in both congeners in response to heat stress, while other changes in the Krebs cycle and the ETC suggest that the production of NADH is decreasing at the highest temperature (Figs 7 and 9). Thus, controlling oxidative damage may depend on the down-regulation of NADH and the up-regulation of NADPH-producing pathways. We observed both: first, a decrease in the levels of key metabolic enzymes linking glycolysis to the Krebs cycle (PDH), of the Krebs cycle itself (mMDH) and the ETC (NADH dehydrogenase and cytochrome *c* reductase), which suggests down-regulation of NADH production, and second, an increase in enzymes that can feed the IDH reaction with substrate (citrate synthase and aspartate amino transferase), suggesting an increased production of NADPH. Such wide-ranging metabolic changes have been shown to occur due to changes in the acetylation status of metabolic enzymes, in part due to the activity of NAD-dependent deacetylases such as sirtuins (Choudhary et al., 2009; North and Sinclair, 2007; Wang et al., 2010; Zhao et al., 2010).

Differences between *Mytilus* congeners in the proteomic response to acute heat stress

In order to compare the responses of the two congeners to heat stress we conducted PCAs that assess the contribution of temperature treatment to the variation in the proteome (Fig. 12). Because we conducted separate PCAs for each species due to limited overlap of proteins in the gel images, the components differ in terms of the variables (e.g. proteins). They include all the proteins that showed a temperature effect (one-way ANOVA) and were subsequently identified (however, similar results were obtained when all proteins were included; data not shown). The temperature treatments (13°C, 24°C, 28°C and 32°C) cluster relative to each other in a similar fashion for each species along component 1, which explains 33.4% and 29.3% of the variation in *M. galloprovincialis* and *M. trossulus*, respectively. Selecting 12 proteins (out of 47 and 61 in *M. galloprovincialis* and *M. trossulus*, respectively) that are the most negatively or positively correlated with the component, the first component is associated with molecular chaperones (sHsps and Hsp70), proteasome isoforms and IDH (more so in *M. galloprovincialis*) in both species. Tubulin (two isoforms), arginine kinase, aspartate amino transferase, nucleoside diphosphate kinase and RhoA are only associated with the first component in *M. galloprovincialis*. Oxidative stress proteins (dihydropteridine reductase and thioredoxin), cytochrome *c* reductase (two isoforms), PDH, F-actin cap protein and Rho-GDI are contributing to the first component in *M. trossulus* only.

The second component, however, separates the 24°C from the 13°C cluster only in *M. galloprovincialis* (Fig. 12). It accounts for 17.5% and 20.4% of the variation in *M. galloprovincialis* and *M. trossulus*, respectively. Selecting the 12 most highly correlated proteins, the component is associated with molecular chaperones (sHsps and Hsp70, three and four isoforms in *M. galloprovincialis* and *M. trossulus*, respectively), pentose–phosphate pathway proteins (two and one isoforms, respectively) and IDH (one isoform) in both species. Proteins contributing only to the component in *M. galloprovincialis* included tubulin (four isoforms), PEPCK and MVP. Proteins unique to *M. trossulus* included the proteasome (two isoforms), NAD-dependent deacetylase (sirtuin 5), glutamine synthetase, protofilament ribbon protein and phenylalanine tRNA synthetase. Taking the number of isoforms into account, molecular chaperones, the proteasome, tubulin and proteins of the pentose–phosphate pathway contribute the most to the differences in the species' second component.

In general, our protein expression as well as the PCA data confirm earlier results on the interspecific differences in Hsp70 synthesis (Hofmann and Somero, 1996a). Although there are broad similarities in the changes in Hsp levels, the more cold-adapted *M. trossulus* showed increasing levels of several (acidic) Hsp70 and sHsp isoforms at lower temperatures in comparison with the more warm-adapted *M. galloprovincialis*. However, they are a number of novel findings of interspecific differences. Several proteasome subunits were decreased in *M. galloprovincialis* but increased in *M. trossulus*, suggesting that differences in protein degradation play important roles in setting thermal limits. The abundance of oxidative stress proteins (aldehyde dehydrogenase, transketolase and thioredoxin) decreased abruptly at 32°C in *M. trossulus* (Figs 2, 3 and 8). Only one putative oxidative stress protein (dihydropteridine reductase) showed higher levels in *M. trossulus* at this temperature. By contrast, *M. galloprovincialis* showed higher levels for three oxidative stress protein isoforms (IDH, SOD and 6-phosphoglucono-lactonase) at 32°C. In addition, the increased abundance of several oxidative stress protein isoforms (transketolase, IDH and SOD) at lower temperatures (24°C and 28°C; Fig. 2) provides further evidence for a potentially more robust response to oxidative stress in *M. galloprovincialis*. Furthermore, although *M. galloprovincialis* increased levels of NADPH-producing proteins, it did not decrease levels of NADH-producing proteins, as did *M. trossulus*. Thus, in *M. trossulus* key oxidative stress proteins showed decreased levels at 32°C while NADH-producing pathways were down-regulated. Together these data suggest that *M. trossulus* may have a lower upper limit (between 28°C and 32°C) than *M. galloprovincialis* (>32°C) to combat heat-induced oxidative stress. Instead it down-regulates NADH-producing pathways to counter the production of ROS through the ETC, possibly at the cost of reduced ATP production (Fig. 11).

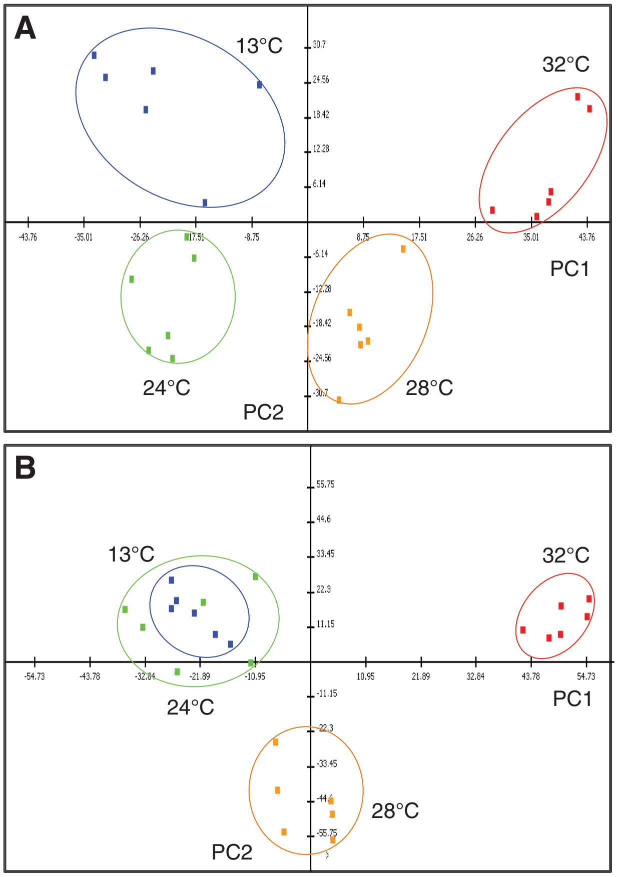

Fig. 12. Principle component analysis of temperature treatments for (A) *Mytilus galloprovincialis* and (B) *Mytilus trossulus*, using proteins that were significant for a main temperature effect (one-way ANOVA, see Figs 2 and 3).

The differences in changing cytoskeletal proteins, e.g. tubulin, between the congeners may be the most important ones, and yet are currently the least understood, because the dynamics of the cytoskeleton in response to heat are poorly described. *Mytilus galloprovincialis* responded to heat stress with increasing abundance of tubulin which later declined at 32°C. In *M. trossulus* most cytoskeleton-associated proteins decreased at 28°C or 32°C. This suggests that the structure of the cytoskeleton was changing differently in response to heat stress in the two congeners, which might explain the interspecific differences in the onset temperature of Hsp70 (acidic isoforms) and sHsp synthesis.

In summary, there are many similarities in the heat shock responses of the two congeners. However, possible differences in protein thermal stability, especially of the cytoskeletal elements, may activate the synthesis of a number of molecular chaperones, (acidic) Hsp70 and some sHsps among the most abundant, at a lower temperature in the cold-adapted *M. trossulus*. Downstream of the activity of molecular chaperones, protein degradation indicated by the abundance of proteasome subunits seems to decrease in *M. galloprovincialis* but increase in *M. trossulus*. Both species respond to heat stress by increasing the abundance of NADPH-producing proteins, possibly facilitating the scavenging of ROS. We hypothesize that *M. trossulus* can respond to heat-induced oxidative stress only up to 28°C and then resorts to the down-regulation of NADH-producing pathways to lower the production of ROS by the ETC. This scenario is not seen in *M. galloprovincialis*, indicating that these systems-level differences in the proteome's response to acute thermal stress may represent some of the molecular factors responsible for the congeners' differences in thermal tolerance.

LIST OF ABBREVIATIONS

AAT	aspartate aminotransferase
cdc42	cell division control protein homolog 42
cMDH	cytosolic malate dehydrogenase
CoA	coenzyme A
EGFR	epidermal growth factor
EST	expressed sequence tag
ETC	electron transport chain
Hsp	heat shock protein
IDH	isocitrate dehydrogenase
IPG	immobilized pH gradient
MAPK	mitogen-activated protein kinase
mMDH	mitochondrial malate dehydrogenase
MOWSE	molecular weight search
MS	mass spectrometry
MVP	major vault protein
NAD(H)	nicotinamide adenine dinucleotide (reduced form)
NADP(H)	nicotinamide adenine dinucleotide phosphate (reduced form)
PCA	principle component analysis
PDH	pyruvate dehydrogenase
PEPCK	phosphoenolpyruvate carboxykinase
pI	isoelectric point
PMF	peptide mass fingerprint
PTM	post-translational modification
ROS	reactive oxygen species
sHsps	small heat shock proteins
SOD	superoxide dismutase
TFA	trifluoroacetic acid
T_{on}	onset temperature
2-D GE	two-dimensional gel electrophoresis

ACKNOWLEDGEMENTS

We thank Daniel D. Magee, Jeremy K. LaBarge, Jacob J. Valenzuela and Brent L. Lockwood for their assistance during the initial experiment. We also thank Brent L. Lockwood and Drs Jennifer Diehl, Peter Fields, Trish Schulte, George Somero, Alexa Tullis and two anonymous reviewers for reading various versions of the manuscript and for providing helpful comments. The study was done in collaboration with Brent Lockwood, Jon Sanders and Dr George Somero (Lockwood et al., 2010). This work was supported by National Science Foundation grant IOS-0717087 to L.T.

REFERENCES

Abele, D., Heise, K., Pörtner, H. O. and Puntarulo, S. (2002). Temperature-dependence of mitochondrial function and production of reactive oxygen species in the intertidal mud clam *Mya arenaria*. *J. Exp. Biol.* **205**, 1831-1841.

Adams, J. C. (2004). Roles of fascin in cell adhesion and motility. *Curr. Opin. Cell Biol.* **16**, 590-596.

Ahn, B. H., Kim, H. S., Song, S., Lee, I. H., Liu, J., Vassilopoulos, A., Deng, C. X. and Finkel, T. (2008). A role for the mitochondrial deacetylase Sirt3 in regulating energy homeostasis. *Proc. Natl. Acad. Sci. USA* **105**, 14447-14452.

Apraiz, I., Mi, J. and Cristobal, S. (2006). Identification of proteomic signatures of exposure to marine pollutants in mussels (*Mytilus edulis*). *Mol. Cell Proteomics* **5**, 1274-1285.

Arrigo, A. P. (2007). The cellular "networking" of mammalian Hsp27 and its functions in the control of protein folding, redox state and apoptosis. In *Molecular Aspects of the Stress Response: Chaperones, Membranes and Networks* (ed. P. Csermely and L. Vígh), pp. 14-26. New York: Springer Science and Business Media.

Berger, W., Steiner, E., Grusch, M., Elbling, L. and Micksche, M. (2009). Vaults and the major vault protein: novel roles in signal pathway regulation and immunity. *Cell. Mol. Life Sci.* **66**, 43-61.

Berth, M., Moser, F. M., Kolbe, M. and Bernhardt, J. (2007). The state of the art in the analysis of two-dimensional gel electrophoresis images. *Appl. Microbiol. Biotechnol.* **76**, 1223-1243.

Bieler, S., Meiners, S., Stangl, V., Pohl, T. and Stangl, K. (2009). Comprehensive proteomic and transcriptomic analysis reveals early induction of a protective anti-oxidative stress response by low-dose proteasome inhibition. *Proteomics* **9**, 3257-3267.

Bourguignon, L. Y., Gilad, E., Rothman, K. and Peyrollier, K. (2005). Hyaluronan-CD44 interaction with IQGAP1 promotes Cdc42 and ERK signaling, leading to actin binding, Elk-1/estrogen receptor transcriptional activation, and ovarian cancer progression. *J. Biol. Chem.* **280**, 11961-11972.

Braby, C. E. and Somero, G. N. (2006a). Ecological gradients and relative abundance of native (*Mytilus trossulus*) and invasive (*M. galloprovincialis*) blue mussels in the California hybrid zone. *Mar. Biol.* **148**, 1249-1262.

Braby, C. E. and Somero, G. N. (2006b). Following the heart: temperature and salinity effects on heart rate in native and invasive species of the blue mussels (genus *Mytilus*). *J. Exp. Biol.* **209**, 2554-2566.

Braun, H. P. and Schmitz, U. K. (1995). Are the 'core' proteins of the mitochondrial bc1 complex evolutionary relics of a processing protease? *Trends Biochem. Sci.* **20**, 171-175.

Burridge, K. and Wennerberg, K. (2004). Rho and Rac take center stage. *Cell* **116**, 167-179.

Chandel, N. S. and Schumacker, P. T. (2000). Cellular oxygen sensing by mitochondria: old questions, new insight. *J. Appl. Physiol.* **88**, 1880-1889.

Choudhary, C., Kumar, C., Gnad, F., Nielsen, M. L., Rehman, M., Walther, T. C., Olsen, J. V. and Mann, M. (2009). Lysine acetylation targets protein complexes and co-regulates major cellular functions. *Science* **325**, 834-840.

Clarkson, M. R., Murphy, M., Gupta, S., Lambe, T., Mackenzie, H. S., Godson, C., Martin, F. and Brady, H. R. (2002). High glucose-altered gene expression in mesangial cells. Actin-regulatory protein gene expression is triggered by oxidative stress and cytoskeletal disassembly. *J. Biol. Chem.* **277**, 9707-9712.

Concannon, C. G., Gorman, A. M. and Samali, A. (2003). On the role of Hsp27 in regulating apoptosis. *Apoptosis* **8**, 61-70.

Cowan, K. J. and Storey, K. B. (2003). Mitogen-activated protein kinases: new signaling pathways functioning in cellular responses to environmental stress. *J. Exp. Biol.* **206**, 1107-1115.

Dada, L. A., Novoa, E., Lecuona, E., Sun, H. and Sznajder, J. I. (2007). Role of the small GTPase RhoA in the hypoxia-induced decrease of plasma membrane Na,K-ATPase in A549 cells. *J. Cell Sci.* **120**, 2214-2222.

Dalle-Donne, I., Rossi, R., Milzani, A., Di Simplicio, P. and Colombo, R. (2001). The actin cytoskeleton response to oxidants: from small heat shock protein phosphorylation to changes in the redox state of actin itself. *Free Radic. Biol. Med.* **31**, 1624-1632.

Diaz-Latoud, C., Buache, E., Javouhey, E. and Arrigo, A. P. (2005). Substitution of the unique cysteine residue of murine Hsp25 interferes with the protective activity of this stress protein through inhibition of dimer formation. *Antioxid. Redox Signal.* **7**, 436-445.

Diz, A. P. and Skibinski, D. O. (2007). Evolution of 2-DE protein patterns in a mussel hybrid zone. *Proteomics* **7**, 2111-2120.

Ellington, W. R. (1989). Phosphocreatine represents a thermodynamic and functional improvement over other muscle phosphagens. *J. Exp. Biol.* **143**, 177-194.

Ellington, W. R. (2001). Evolution and physiological roles of phosphagen systems. *Annu. Rev. Physiol.* **63**, 289-325.

Fields, P. A., Rudomin, E. L. and Somero, G. N. (2006). Temperature sensitivities of cytosolic malate dehydrogenases from native and invasive species of marine mussels (genus *Mytilus*): sequence-function linkages and correlations with biogeographic distribution. *J. Exp. Biol.* **209**, 656-667.

Finkel, T., Deng, C. X. and Mostoslavsky, R. (2009). Recent progress in the biology and physiology of sirtuins. *Nature* **460**, 587-591.

Geller, J. B. (1999). Decline of a native mussel masked by sibling species invasion. *Conserv. Biol.* **13**, 661-664.

Glickman, M. H. and Ciechanover, A. (2002). The ubiquitin-proteasome proteolytic pathway: destruction for the sake of construction. *Physiol. Rev.* **82**, 373-428.

Go, Y. M. and Jones, D. P. (2008). Redox compartmentalization in eukaryotic cells. *Biochim. Biophys. Acta* **1780**, 1273-1290.

Gracey, A. Y., Chaney, M. L., Boomhower, J. P., Tyburczy, W. R., Connor, K. and Somero, G. N. (2008). Rhythms of gene expression in a fluctuating intertidal environment. *Curr. Biol.* **18**, 1501-1507.

Harley, C. D. G., Hughes, A. R., Hultgren, K., Miner, B. G., Sorte, C. J. B., Thornber, C. S., Rodrigues, L. F., Tomanek, L. and Williams, S. L. (2006). The impacts of climate change in coastal marine systems. *Ecol. Lett.* **9**, 228-241.

Haslbeck, M., Franzmann, T., Weinfurtner, D. and Buchner, J. (2005). Some like it hot: the structure and function of small heat-shock proteins. *Nat. Struct. Mol. Biol.* **12**, 842-846.

Hinchcliffe, E. H. and Linck, R. W. (1998). Two proteins isolated from sea urchin sperm flagella: structural components common to the stable microtubules of axonemes and centrioles. *J. Cell Sci.* **111**, 585-595.

Hochachka, P. W. and Somero, G. N. (2002). *Biochemical Adaptation: Mechanism and Process in Physiological Evolution.* Oxford: Oxford University Press.

Hofmann, G. E. and Somero, G. N. (1996a). Interspecific variation in thermal denaturation of proteins in the congeneric mussels *Mytilus trossulus* and *M. galloprovincialis*: evidence from the heat-shock response and protein ubiquitination. *Mar. Biol.* **126**, 65-75.

Hofmann, G. E. and Somero, G. N. (1996b). Protein ubiquitination and stress protein synthesis in *Mytilus trossulus* occurs during recovery from tidal emersion. *Mol. Mar. Biol. Biotechnol.* **5**, 175-184.

Holcik, M. and Sonenberg, N. (2005). Translational control in stress and apoptosis. *Nat. Rev. Mol. Cell Biol.* **6**, 318-327.

Huot, J., Houle, F., Spitz, D. R. and Landry, J. (1996). HSP27 phosphorylation-mediated resistance against actin fragmentation and cell death induced by oxidative stress. *Cancer Res.* **56**, 273-279.

Huot, J., Houle, F., Marceau, F. and Landry, J. (1997). Oxidative stress-induced actin reorganization mediated by the p38 mitogen-activated protein kinase/heat shock protein 27 pathway in vascular endothelial cells. *Circ. Res.* **80**, 383-392.

Huot, J., Houle, F., Rousseau, S., Deschesnes, R. G., Shah, G. M. and Landry, J. (1998). SAPK2/p38-dependent F-actin reorganization regulates early membrane blebbing during stress-induced apoptosis. *J. Cell Biol.* **143**, 1361-1373.

IPCC (2007). *Climate Change 2007 – The Physical Science Basis.* Cambridge: Cambridge University Press.

Jakob, U., Muse, W., Eser, M. and Bardwell, J. C. (1999). Chaperone activity with a redox switch. *Cell* **96**, 341-352.

Jo, S. H., Son, M. K., Koh, H. J., Lee, S. M., Song, I. H., Kim, Y. O., Lee, Y. S., Jeong, K. S., Kim, W. B., Park, J. W. et al. (2001). Control of mitochondrial redox balance and cellular defense against oxidative damage by mitochondrial NADP$^+$-dependent isocitrate dehydrogenase. *J. Biol. Chem.* **276**, 16168-16176.

Kolch, W. (2005). Coordinating ERK/MAPK signalling through scaffolds and inhibitors. *Nat. Rev. Mol. Cell Biol.* **6**, 827-837.

Kültz, D. (2005). Molecular and evolutionary basis of the cellular stress response. *Annu. Rev. Physiol.* **67**, 225-257.

Lavoie, J. N., Lambert, H., Hickey, E., Weber, L. A. and Landry, J. (1995). Modulation of cellular thermoresistance and actin filament stability accompanies phosphorylation-induced changes in the oligomeric structure of heat shock protein 27. *Mol. Cell. Biol.* **15**, 505-516.

Law, I. K., Liu, L., Xu, A., Lam, K. S., Vanhoutte, P. M., Che, C. M., Leung, P. T. and Wang, Y. (2009). Identification and characterization of proteins interacting with SIRT1 and SIRT3: implications in the anti-aging and metabolic effects of sirtuins. *Proteomics* **9**, 2444-2456.

Lee, Y. J., Cho, H. N., Jeoung, D. I., Soh, J. W., Cho, C. K., Bae, S., Chung, H. Y., Lee, S. J. and Lee, Y. S. (2004). HSP25 overexpression attenuates oxidative stress-induced apoptosis: roles of ERK1/2 signaling and manganese superoxide dismutase. *Free Radic. Biol. Med.* **36**, 429-444.

Liang, P. and MacRae, T. H. (1997). Molecular chaperones and the cytoskeleton. *J. Cell Sci.* **110**, 1431-1440.

Lin, S. J., Ford, E., Haigis, M., Liszt, G. and Guarente, L. (2004). Calorie restriction extends yeast life span by lowering the level of NADH. *Genes Dev.* **18**, 12-16.

Lockwood, B. L., Sanders, J. G. and Somero, G. N. (2010). Transcriptomic responses to heat stress in invasive and native blue mussels (genus *Mytilus*): molecular correlates of invasive success. *J. Exp. Biol.* **213**, 3548-3558.

López, J. L., Marina, A., Vázquez, J. and Alvarez, G. (2002). A proteomic approach to the study of marine mussels *Mytilus edulis* and *M. galloprovincialis*. *Mar. Biol.* **141**, 217-223.

Luedeking, A. and Koehler, A. (2004). Regulation of expression of multixenobiotic resistance (MXR) genes by environmental factors in the blue mussel *Mytilus edulis*. *Aquat. Toxicol.* **69**, 1-10.

Marks, F., Klingmüller, U. and Müller-Decker, K. (2009). *Cellular Signal Processing: an Introduction to the Molecular Mechanisms of Signal Transduction.* New York: Garland Science, Taylor and Francis Group.

Martinez-Fernandez, M., Rodriguez-Pineiro, A. M., Oliveira, E., Paez de la Cadena, M. and Rolan-Alvarez, E. (2008). Proteomic comparison between two marine snail ecotypes reveals details about the biochemistry of adaptation. *J. Proteome Res.* **7**, 4926-4934.

McDonagh, B. and Sheehan, D. (2007). Effect of oxidative stress on protein thiols in the blue mussel *Mytilus edulis*: proteomic identification of target proteins. *Proteomics* **7**, 3395-3403.

McDonald, J. H. and Koehn, R. K. (1988). The mussels *Mytilus galloprovincialis* and *Mytilus trossulus* on the Pacific coast of North America. *Mar. Biol.* **99**, 111-118.

Murphy, M. P. (2009). How mitochondria produce reactive oxygen species. *Biochem. J.* **417**, 1-13.

Nadeau, S. I. and Landry, J. (2007). Mechanisms of activation and regulation of the heat shock-sensitive signaling pathways. In *Molecular Aspects of the Stress Response: Chaperones, Membranes and Networks* (ed. P. Csermely and L. Vígh), pp. 100-113. New York: Springer Science and Business Media.

Nelson, D. L. and Cox, M. M. (2008). *Lehninger Principles of Biochemistry.* New York: W. H. Freeman and Company.

Norris, C. E. and Hightower, L. E. (2002). Discovery of two distinct small heat shock protein (HSP) families in the desert fish *Poeciliopsis*. *Prog. Mol. Subcell. Biol.* **28**, 19-35.

North, B. J. and Sinclair, D. A. (2007). Sirtuins: a conserved key unlocking AceCS activity. *Trends Biochem. Sci.* **32**, 1-4.

Parmesan, C. (2006). Ecological and evolutionary responses to recent climate change. *Annu. Rev. Ecol. Evol. Syst.* **37**, 637-669.

Place, S. P., O'Donnell, M. J. and Hofmann, G. E. (2008). Gene expression in the intertidal mussel *Mytilus californianus*: physiological response to environmental factors on a biogeographic scale. *Mar. Ecol. Progr. Ser.* **356**, 1-14.

Podrabsky, J. E. and Somero, G. N. (2004). Changes in gene expression associated with acclimation to constant temperatures and fluctuating daily temperatures in an annual killifish *Austrofundulus limnaeus*. *J. Exp. Biol.* **207**, 2237-2254.

Ponzone, A., Spada, M., Ferraris, S., Dianzani, I. and de Sanctis, L. (2004). Dihydropteridine reductase deficiency in man: from biology to treatment. *Med. Res. Rev.* **24**, 127-150.

Pörtner, H. O. (2002). Climate variations and the physiological basis of temperature dependent biogeography: systemic to molecular hierarchy of thermal tolerance in animals. *Comp. Biochem. Physiol. A Physiol.* **132**, 739-761.

Pörtner, H. O. and Knust, R. (2007). Climate change affects marine fishes through the oxygen limitation of thermal tolerance. *Science* **315**, 95-97.

Salway, J. G. (2004). *Metabolism at a Glance.* Oxford: Blackwell Publishing Limited.

Sanders, B. M., Hope, C., Pascoe, V. M. and Martin, L. S. (1991). Characterization of stress protein response in two species of *Colisella* limpets with different temperature tolerances. *Physiol. Zool.* **64**, 1471-1489.

Schlicker, C., Gertz, M., Papatheodorou, P., Kachholz, B., Becker, C. F. and Steegborn, C. (2008). Substrates and regulation mechanisms for the human mitochondrial sirtuins Sirt3 and Sirt5. *J. Mol. Biol.* **382**, 790-801.

Schneider, K. R. (2008). Heat stress in the intertidal: comparing survival and growth of an invasive and native mussel under a variety of thermal conditions. *Biol. Bull.* **215**, 253-264.

Schneider, K. R. and Helmuth, B. (2007). Spatial variability in habitat temperature may drive patterns of selection between an invasive and native mussel species. *Mar. Ecol. Prog. Ser.* **339**, 157-167.

Schwer, B. and Verdin, E. (2008). Conserved metabolic regulatory functions of sirtuins. *Cell Metab.* **7**, 104-112.

Seed, R. (1992). Systematics, evolution and distribution of mussels belonging to the genus *Mytilus*: an overview. *Am. Malacol. Bull.* **117**, 123-137.

Setter, P. W., Malvey-Dorn, E., Steffen, W., Stephens, R. E. and Linck, R. W. (2006). Tektin interactions and a model for molecular functions. *Exp. Cell Res.* **312**, 2880-2896.

Shick, J. M., Widdows, J. and Gnaiger, E. (1988). Calorimetric studies of behavior, metabolism and energectics of sessile intertidal animals. *Am. Zool.* **28**, 161-181.

Somero, G. N. (2010). The physiology of climate change: how potentials for acclimatization and genetic adaptation will determine "winners" and "losers". *J. Exp. Biol.* **213**, 912-920.

Stillman, J. H. (2003). Acclimation capacity underlies susceptibility to climate change. *Science* **301**, 65.

Stillman, J. H. and Tagmount, A. (2009). Seasonal and latitudinal acclimatization of cardiac transcriptome responses to thermal stress in porcelain crabs, *Petrolisthes cinctipes*. *Mol. Ecol.* **18**, 4206-4226.

Sugano, Y. (2009). DyP-type peroxidases comprise a novel heme peroxidase family. *Cell. Mol. Life Sci.* **66**, 1387-1403.

Suprenant, K. A., Bloom, N., Fang, J. and Lushington, G. (2007). The major vault protein is related to the toxic anion resistance protein (TelA) family. *J. Exp. Biol.* **210**, 946-955.

Tell, G. (2006). Early molecular events during response to oxidative stress in human cells by differential proteomics. In *Redox Proteomics: from Protein Modifications to Cellular Dysfunction and Diseases* (ed. I. Dalle-Donne, A. Scaloni and D. A. Butterfield), pp. 369-562. Hoboken, New Jersey: John Wiley and Sons Incorporated.

Teranishi, K. S. and Stillman, J. H. (2007). A cDNA microarray analysis of the response to heat stress in hepatopancreas tissue of the porcelain crab *Petrolisthes cinctipes*. *Comp. Biochem. Physiol. D Genomics Proteomics* **2**, 53-62.

Tomanek, L. (2005). Two-dimensional gel analysis of the heat-shock response in marine snails (genus *Tegula*): interspecific variation in protein expression and acclimation ability. *J. Exp. Biol.* **208**, 3133-3143.

Tomanek, L. (2008). The importance of physiological limits in determining biogeographical range shifts due to global climate change: the heat-shock response *Physiol. Biochem. Zool.* **81**, 709-717.

Tomanek, L. (2010). Variation in the heat shock response and its implication for predicting the effect of global climate change on species' bioegographic distribution ranges and metabolic costs. *J. Exp. Biol.* **213**, 971-979.

Tomanek, L. and Somero, G. N. (1999). Evolutionary and acclimation-induced variation in the heat-shock responses of congeneric marine snails (genus *Tegula*) from different thermal habitats: implications for limits of thermotolerance and biogeography. *J. Exp. Biol.* **202**, 2925-2936.

Wang, Q., Zhang, Y., Yang, C., Xiong, H., Lin, Y., Yao, J., Li, H., Xie, L., Zhao, W., Yao, Y. et al. (2010). Acetylation of metabolic enzymes coordinates carbon source utilization and metabolic flux. *Science* **327**, 1004-1007.

Westerheide, S. D., Anckar, J., Stevens, S. M., Jr, Sistonen, L. and Morimoto, R. I. (2009). Stress-inducible regulation of heat shock factor 1 by the deacetylase SIRT1. *Science* **323**, 1063-1066.

Zhao, S., Xu, W., Jiang, W., Yu, W., Lin, Y., Zhang, T., Yao, J., Zhou, L., Zeng, Y., Li, H. et al. (2010). Regulation of cellular metabolism by protein lysine acetylation. *Science* **327**, 1000-1004.

Zwaan, A. D. and Mathieu, M. (1992). Cellular biochemistry and endocrinology. In *The Mussel Mytilus: Ecology, Physiology, Genetics and Culture* (ed. E. Gosling), pp. 223-307. Amsterdam, London, New York, Tokyo: Elsevier.